Acta Pharmaceutica Sinica B 2019;9(5):880–901

Chinese Pharmaceutical Association
Institute of Materia Medica, Chinese Academy of Medical Sciences

Acta Pharmaceutica Sinica B

www.elsevier.com/locate/apsb
www.sciencedirect.com

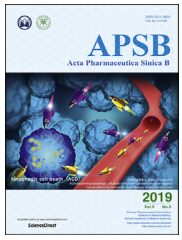

REVIEW

# Structural simplification: an efficient strategy in lead optimization

**Shengzheng Wang**[a,b], **Guoqiang Dong**[a,*], **Chunquan Sheng**[a,*]

[a]*Department of Medicinal Chemistry, School of Pharmacy, Second Military Medical University, Shanghai 200433, China*
[b]*Department of Medicinal Chemistry and Pharmaceutical Analysis, School of Pharmacy, Fourth Military Medical University, Xi'an 710032, China*

Received 5 March 2019; received in revised form 4 May 2019; accepted 15 May 2019

**KEY WORDS**

Structural simplification;
Lead optimization;
Drug discovery;
Drug design;
Reducing rings number;
Reducing chiral centers;
Structure-based simplification;
Pharmacophore-based simplification

**Abstract** The trend toward designing large hydrophobic molecules for lead optimization is often associated with poor drug-likeness and high attrition rates in drug discovery and development. Structural simplification is a powerful strategy for improving the efficiency and success rate of drug design by avoiding "molecular obesity". The structural simplification of large or complex lead compounds by truncating unnecessary groups can not only improve their synthetic accessibility but also improve their pharmacokinetic profiles, reduce side effects and so on. This review will summarize the application of structural simplification in lead optimization. Numerous case studies, particularly those involving successful examples leading to marketed drugs or drug-like candidates, will be introduced and analyzed to illustrate the design strategies and guidelines for structural simplification.



*Abbreviations:* 3D, three-dimensional; 11$\beta$-HSD, 11$\beta$-hydroxysteroid dehydrogenase; aaRSs, aminoacyl-tRNA synthetases; aa-AMP, aminoacyl-AMP; aa-AMS, aminoacylsulfa-moyladenosine; ADMET, absorption, distribution, metabolism, excretion and toxicity; AM2, adrenomedullin-2 receptor; BIOS, biology-oriented synthesis; CCK, cholecystokinin receptor; CGRP, calcitonin gene-related peptide; GlyT1, glycine transport 1; $hA_3$ AR, human A3 adenosine receptor; HBV, hepatitis B virus; HDAC, histone deacetylase; HLM, human liver microsome; JAKs, Janus tyrosine kinases; LE, ligand efficiency; LeuRS, leucyl-tRNA synthetase; MCRs, multicomponent reactions; MDR-TB, multidrug-resistant tuberculosis; mTORC1, mammalian target of rapamycin complex 1; MW, molecular weight; NP, natural product; NPM, nucleophosmin; PD, pharmacodynamic; PK, pharmacokinetic; PKC, protein kinase C; SAHA, vorinostat; SAR, structure–activity relationship; SCONP, structural classification of natural product; TSA, trichostatin A; ThrRS, threonyl-tRNA synthetase; *Tb*LeuRS, *T. brucei* LeuRS; VANGL1, van-Gogh-like receptor protein 1.

*Corresponding authors. Tel./fax: +86 21 81871242 (Guoqiang Dong); Tel./fax: +86 21 81871239 (Chunquan Sheng).
E-mail addresses: dgq-81@163.com (Guoqiang Dong), shengcq@smmu.edu.cn (Chunquan Sheng).

Peer review under responsibility of Institute of Materia Medica, Chinese Academy of Medical Sciences and Chinese Pharmaceutical Association.

https://doi.org/10.1016/j.apsb.2019.05.004

## 1. Introduction

For several decades, the pharmaceutical industry has suffered high attrition rates in drug development despite an ever-increasing understanding of chemistry and biology and the emergence of new drug discovery technologies[1,2]. A typical drug discovery and development process includes target identification, hit generation, hit-to-lead-to-candidate optimization, and preclinical and clinical evaluation of the resulting drug candidates. The efficiency of the hit-to-lead-to-candidate process is particularly important for identifying drug-like candidates and determining the success of the drug development process[3]. During hit-to-lead optimization, medicinal chemists always attempt to improve the target binding affinity and maximize the *in vitro* potency. This usually leads to compounds with higher molecular weights (MW values) and lipophilicities, resulting in undesirable physicochemical properties and pharmacokinetic properties. A retrospective analysis of molecules reported in the *Journal of Medicinal Chemistry* from 1959 to 2009 indicated that the reported bioactive molecules became larger, more complex, more lipophilic, flatter and more aromatic[4]. Oprea et al[5]. analyzed a dataset of lead-drug pairs and found that in the optimization of a lead into a drug, the structural complexity of the compound generally increased. During the hit-to-lead-to-candidate process, the MW, lipophilicity, and number of rings and rotatable bonds will increase[6]. However, this trend increases the failure rate of drug development due to the poor ADMET (absorption, distribution, metabolism, excretion and toxicity) profiles of the resulting candidates.

"Molecular obesity" has been considered an important reason for the high attrition rates of drug candidates and low productivity in the pharmaceutical industry[1,7,8]. Additionally, Polanski's analysis revealed that less complex drugs were more likely to achieve better market success[2]. Currently, multivariate optimization, namely, simultaneous optimization of the pharmacological and pharmacokinetic properties, has been widely used to improve the efficiency of lead optimization[9]. To reduce molecular obesity, structural simplification by the judicious removal of nonessential groups, represents a practical and powerful strategy in multivariate lead optimization.

Molecular obesity is associated with large MW and high molecular complexity. In particular, the molecular complexity of target molecules should be analyzed before structural simplification of the design (Fig. 1). The number of rings and how they are connected (linked, fused or bridged) as well as the number and configuration of chiral centers are key factors in determining the molecular complexity[10]. Reducing the MW and molecular complexity has been regarded as having positive effects on the pharmacokinetic (PK)/pharmacodynamics (PD) profiles[11,12]. The typical process for structural simplification to generate simplified analogues mainly includes a step-by-step analysis of the complex structure, a determination of the substructures (or groups) important for the biological activity, the elucidation of the structure–activity relationships (SARs) and pharmacophores, and the removal of unnecessary structural motifs. Eliminating redundant chiral centers and reducing the number of rings are the most widely used approaches to simplification[13,14]. The efficiency of the structural simplification process will be improved if the targets and binding mode of the lead compounds have been identified. The effects of key structural motifs on the ligand–target interactions will guide the rational design of simplified derivatives.

Due to its importance in drug discovery, herein we present a comprehensive review of structural simplification in medicinal chemistry and drug discovery. Representative examples leading to marketed drugs or drug-like molecules will be introduced and analyzed in detail to illustrate the design strategies and guidelines associated with structural simplification.

## 2. Structural simplification of natural products

Natural products (NPs) are rich resources for drug discovery and development[13,15]. However, the complex chemical structures of NPs often complicate the total synthesis, SAR investigations and structural optimizations and result in unfavorable ADMET properties[16]. Therefore, simplifying complex structures without decreasing the desired biological activity is an effective strategy for improving synthetic accessibility and accelerating the drug development process. A classic example of the structural simplification of NPs is the development of simplified morphine-derived analgesics, in which the complex pentacyclic system of morphine (**1**) was simplified step-by-step (Fig. 2)[17]. Systemically reducing the complexity of the ring system led to a number of semisynthetic or synthetic analgesics (*e.g.,* compounds **2**–**5**)[18–20]. The

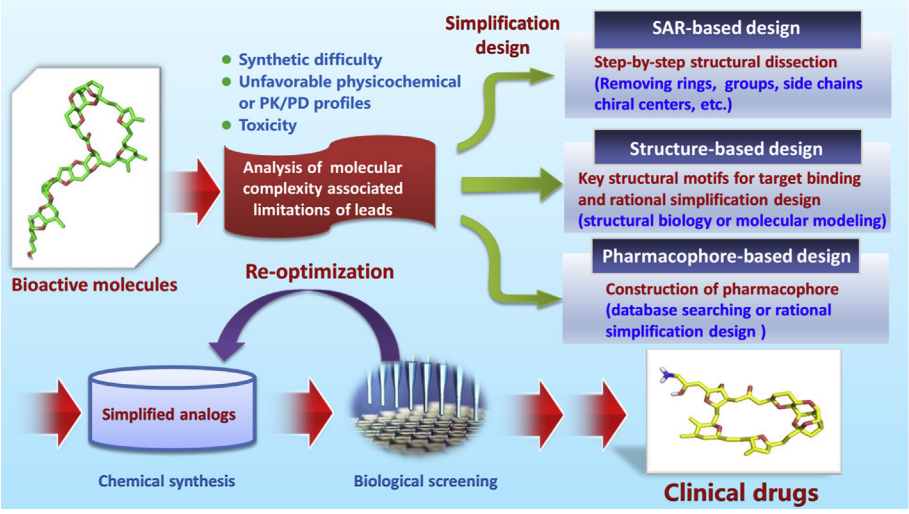


**Figure 1** A general process for the structural simplification of bioactive molecules.

successful development of simplified morphine derivatives also provides several principles for further structural simplifications. First, reducing the scaffold complexity and removing chiral centers are effective approaches for designing simplified molecules. Second, retaining the key pharmacophores (for morphine: an aromatic ring, a basic tertiary amine and a piperidine or piperidine-mimic) and proper conformation is essential for biological activity. Third, the pharmacological and toxicological properties may change during the structural simplification process. Compared with morphine, several simplified morphine analogues (*e.g.,* butophanol[19−21], **2**) show improved potency and reduced addiction side effects[22−27]. Morphine is mainly a $\mu$-opioid receptor agonist ($K_i$ = 1.8 nmol/L)[28], whereas pentazocine (**3**) is a $\kappa$-opioid receptor agonist and μ-receptor antagonist[21].

### 2.1. *Marketed drugs and clinical candidates derived from the structural simplification of NPs*

The successful development of simplified morphine derivatives inspired numerous structural simplification investigations based on NPs[29]. Herein, only the case studies leading to marketed drugs and clinical candidates are briefly discussed (Figs. 3 and 4).

Halichondrin B (**6**, Fig. 3) is a very complex marine NP[30] that acts by destabilizing tubulin, and it shows excellent antitumor activity[31,32]. However, drug development of halichondrin B was hampered by the scarcity of the marine source and its difficult total synthesis[33] (approximately 120 steps). SAR analysis indicated that the C1−C38 macrolide-truncated fragment showed comparable antitumor activity to that of halichondrin B, and the unstable lactone moiety could be replaced by a nonhydrolyzable ketone[34]. Thus, the simplified analogue eribulin mesilate (**7**, Fig. 3) was successfully developed for the treatment of refractory metastatic breast cancer[35−37].

Myriocin (**8**, Fig. 3) is a fungal metabolite with immunosuppressive activity ($IC_{50}$ = 8.0 nmol/L) that acts by targeting sphingosine-1-phosphate (S1P) receptors[38]. Myriocin was unsuitable for direct clinical development because of its significant toxicity and poor solubility. The structural simplification of myriocin was based on the SAR that the C-4 hydroxyl group, C-6 double bond, C-14 ketone and C-3 chiral center were unnecessary for the activity[38,39]. Thus, simplified analogue fingolimod (**9**, Fig. 3) was designed with a symmetric 2-alkyl-2-aminopropane-1,3-diol side chain to mimic the terminal structure of sphingosine, and the incorporation of a phenyl group reduced the flexibility of the alkyl side chain[38,40]. Compared with myriocin, fingolimod showed higher potency ($IC_{50}$ = 6.1 nmol/L), more favorable physicochemical properties and reduced toxicity, and in 2010, it was marketed for the treatment of multiple sclerosis.

The first marketed histone deacetylase (HDAC) inhibitor, vorinostat (SAHA, **11**, Fig. 3) can be regarded as a simplified analogue of trichostatin A[41] (TSA, **10**, Fig. 3). The *trans*-conjugated double bonds and the chiral center in TSA were found to have little impact on its HDAC-inhibitory activity. After eliminating the chiral center and the conjugated double bond, simplified analogue SAHA retained the excellent HDAC-inhibitory activity (HDAC1 $IC_{50}$ = 0.04 μmol/L)[42] and can be easily synthesized[43]. SAHA was approved by FDA in 2006 for the treatment of advanced primary cutaneous T-cell lymphoma[44].

Schisandin C (**12**, Fig. 3) is a NP with anti-hepatitis B virus (HBV) and transaminase-decreasing activities[45]. Structural simplification studies were initiated by the total synthesis of an incorrectly assigned structure of schisandin C. Interestingly, a synthetic intermediate (bifendate) was found to potently decrease aminotransferase levels[46]. After structural optimization, bicyclol (**13**) was successfully developed for treating patients with elevated aminotransferase levels caused by chronic hepatitis[45]. Compared with schisandin C, bicyclol retains the potent pharmacological activity, and its solubility and pharmacokinetic properties are greatly improved[47]. Moreover, the synthetic challenge is greatly decreased due to the removal of the seven-membered ring.

Currently, examples of clinical candidates derived from the structural simplification of NPs are rather limited (Fig. 4). Staurosporine (**14**) is a potent inhibitor of protein kinase C (PKC). Structural simplification of staurosporine led to the discovery of two clinical candidates, ruboxistaurin (**15**)[48] and enzastaurin (**16**)[49], which have both entered phase III clinical trials. However, further drug development failed because of limited efficacy. Asperlicin (**17**) is a selective antagonist ($IC_{50}$ = 1.4 μmol/L) of cholecystokinin receptors (CCK) with potential therapeutic effects in CCK-related gastrointestinal disorders[50,51]. To address the limitations of asperlicin (*e.g.,* challenging total synthesis and poor oral bioavailability), simplified analogue devazepide (**18**,

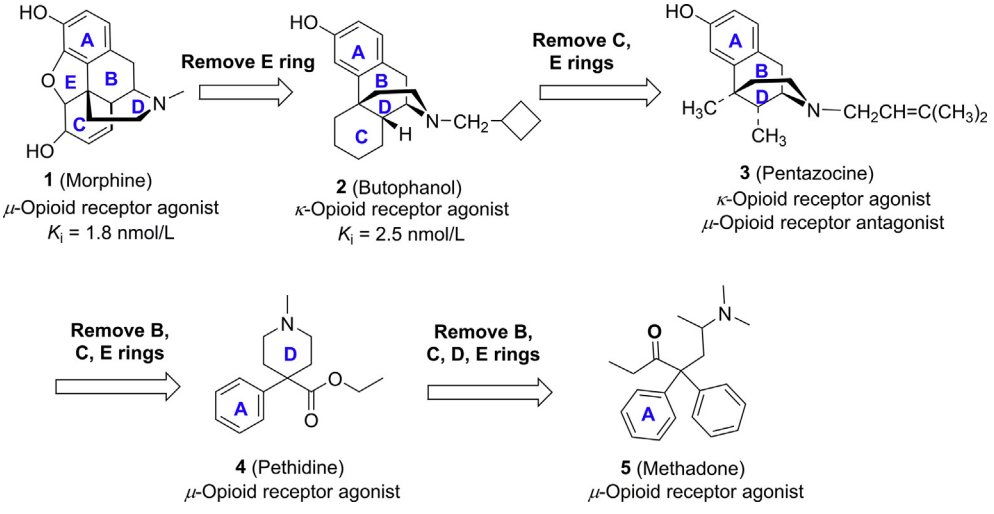


**Figure 2** Structural simplification of morphine leading to marketed drugs including butophanol, pentazocine, pethidine and methadone.

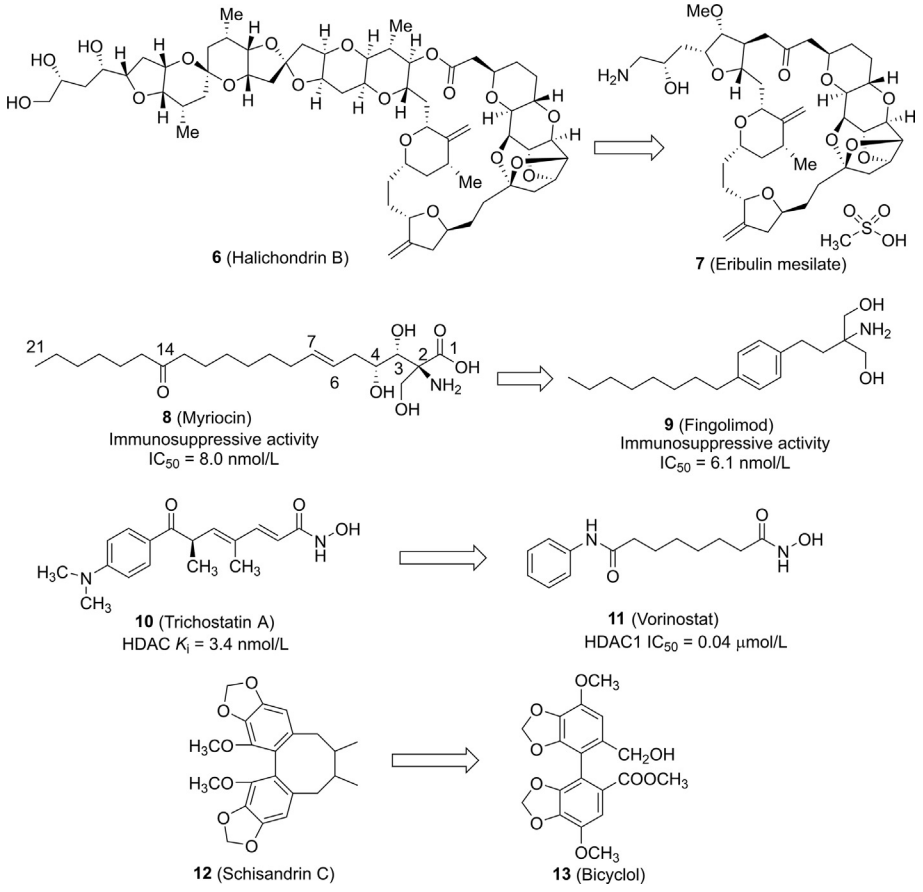


**Figure 3** Structural simplification of natural products (NPs) leading to marketed drugs including eribulin mesilate, fingolimod, vorinostat and bicyclol.

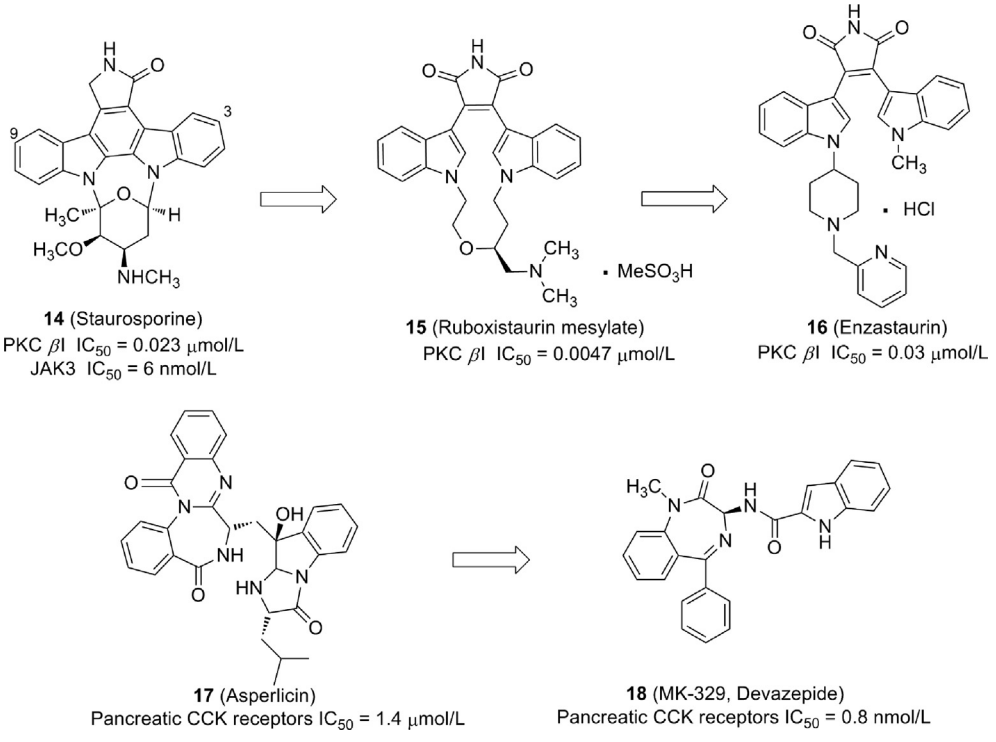


**Figure 4** Structural simplification of NPs leading to clinical candidates including ruboxistaurin, enzastaurin and devazepide.

MK-329) was developed, and it shows excellent CCK antagonistic activity ($IC_{50}$ = 0.8 nmol/L) and selectivity[52−54]. Although the clinical development of devazepide was not successful, it is widely used as a reference compound in studies on CCK receptors. In most of these case studies, reducing the synthetic difficulty is the initial impetus for the structural simplification of the NP, and in this context, simplifying the scaffold ring system and eliminating chiral centers are the most frequently used approaches. When the NPs are simpler, more favorable PK/PD profiles can be achieved.

### 2.2. *New synthetic and computational approaches in the structural simplification of NPs*

#### 2.2.1. *Structural simplification of bioactive alkaloids via multicomponent reactions*

Multicomponent reactions (MCRs) have attracted great interest in medicinal chemistry and drug discovery due to their synthetic advantages, such as their environmental friendliness, atom economy, and ability to generate complex molecules in only one or two synthetic steps[55]. One-step MCRs have been successfully used to construct simplified analogues of NPs (*e.g.,* podophyllotoxin[56], campothecin[57] and melicobisquinolinone B[58]).

4*H*-Pyrano-[2,3-*b*]naphthoquinone (blue part, Fig. 5) is a structural motif commonly found in NPs, such as pyranokunthone B (**19**)[59], lapachones (**20**−**21**)[60], and rhinacanthin O (**22**)[61]. Magedov et al.[62] developed a three-component reaction of 2-hydroxy-1,4-naphthoquinone (**23**) with malononitrile (**25**) and various aromatic aldehydes (**24**) to efficiently construct a library of compounds with simplified pyranonaphthoquinone scaffolds (**26**, Fig. 5). Most derivatives displayed low micromolar inhibitory activities against a wide range of cancer cell lines. Compounds **27** and **28** displayed potent antitumor activities against HeLa cells with $GI_{50}$ values of 4.0 and 5.3 μmol/L, respectively, which were comparable to that of *β*-lapachone (**21**, $GI_{50}$ = 4.6 μmol/L).

#### 2.2.2. *Computational fragmentation of NPs*

Recently, there has been growing interest in the computational analysis of NPs using cheminformatic and bioinformatic tools[16]. The stepwise deconstruction of NPs leads to simplified derivatives called NP fragments[13]. The NP-derived fragments have obvious advantages in drug discovery due to their reduced structural complexity, good synthetic accessibility and improved drug-likeness. For example, Waldmann's group performed cheminformatic analysis on more than 180,000 NPs and assembled a library containing 2000 structurally diverse NP-derived fragments[63]. The utility of their fragment library was demonstrated by the identification of novel p38a MAP kinase stabilizers (**29**) and phosphatase inhibitors (**30**−**35**) with high ligand efficiency (LE) values (Fig. 6)[63].

The sequential dissection of NPs also offers new opportunities to discover novel biologically active chemical scaffolds. Thus, NP fragments can be used as good starting points for chemical biology and medicinal chemistry studies[64]. The incorporation of NP-derived fragments has been validated as an effective strategy in drug design. More importantly, these fragments may retain the unique structural features and biological relevance of their parent NPs, which have a high degree of three-dimensional (3D) organization and occupy largely unexplored chemical space[65,66]. Thus, NP fragments should be particularly useful in fragment-based drug design[67], *de novo* drug design[68] and discovering small-molecule inhibitors of challenging protein targets (*e.g.,* protein−protein interactions)[69].

Initially, the fragmentation of NPs was driven by chemistry-based rules, such as the structural classification of NPs (SCONP)[70]. Sequential structural simplifications following the SCONP result in a scaffold tree in which the complexity of the scaffold decreases step-by-step (Fig. 7)[71]. The simpler scaffolds in the scaffold tree may retain the bioactivity of the more complex compounds, and they can then be used for drug design or designing compound libraries. A typical SCONP scaffold tree starting from 11*β*-hydroxysteroid dehydrogenases (11*β*-HSDs) inhibitors glycyrrhetinic acid (**36**) and dysidiolide (**37**) is depicted in Fig. 7[70,72]. Inspired by the simplified scaffolds, libraries of *α*,*β*-unsaturated *γ*-lactones (**38**−**39**) and dehydrodecalines (**40**) were synthesized and assayed. A very simple compound (**41**) showed good and selective activity against 11*β*-HSD1 ($IC_{50}$ = 0.35 μmol/L).

As an improved version of SCONP, Waldmann's group further developed Scaffold Hunter, an interactive tool for the intuitive hierarchical analysis of complex structures and bioactivity data[73,74]. Unlike SCONP, bioactivity was used as a major criterion for guiding the hierarchical arrangement. Thus, Scaffold Hunter

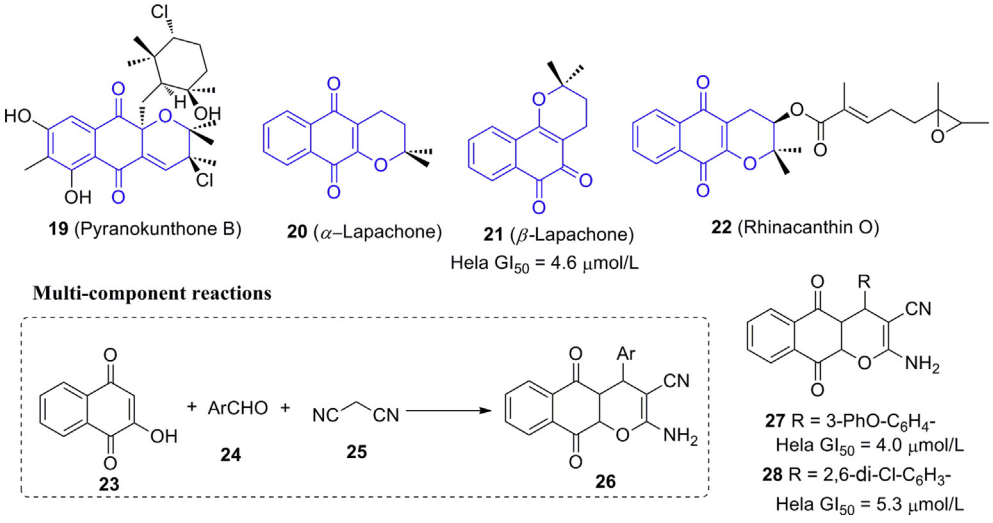


**Figure 5** Structural simplification of pyrano-naphthoquinone NPs based on multi-component reactions (MCRs).

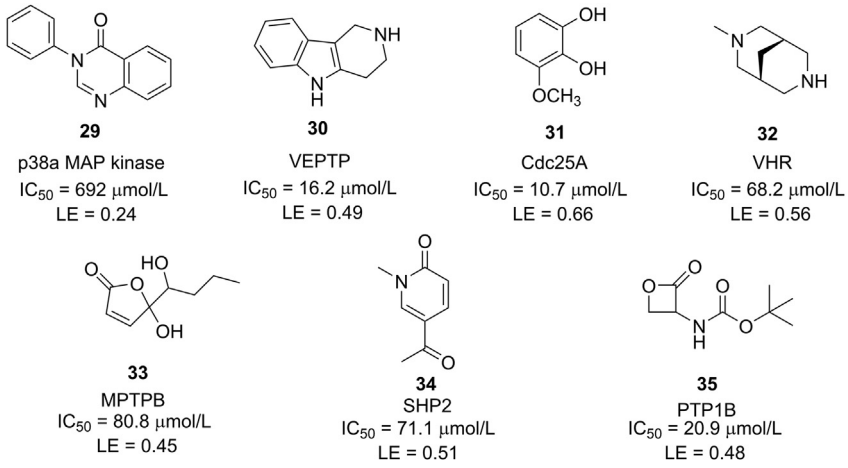


**Figure 6** Selected examples of bioactive NP fragments. Abbreviations: mycobacterium tuberculosis protein tyrosine phosphatases B (MPTPB), vascular endothelial protein tyrosine phosphatase (VEPTP), cell division cycle 25 homologue A (Cdc25A), VH1-related phosphatase (VHR), SH2 domain-containing phosphatase (SHP2) and protein tyrosine phosphatase 1B (PTP1B).

generates a hierarchical scaffold tree annotated with bioactivity information. Scaffold Hunter enables the rapid and efficient navigation of large chemical and biological spaces and the identification of virtual (or novel) scaffolds possessing bioactivities similar to those of the original NPs. These virtual scaffolds offer unique opportunities to discover new ligands for a particular protein target or compounds that can be used as molecular probes to identify novel drug targets. Notably, complex structures can be simplified into synthetically accessible bicyclic to tetracyclic scaffolds with retained bioactivity, and these smaller structures offer improved drug-likeness and synthetically accessible starting points for designing new bioactive chemotypes. Recently, Prescher et al[75]. constructed a library of unique NP-like fragments that covers novel and unprecedented chemical space by the degradation and diversification of NPs.

### 2.2.3. *Biology-oriented synthesis*

As hypothesis-generating approaches, SCONP and Scaffold Hunter laid a foundation for the design of collections of structurally simplified NP-like compounds[65]. Waldmann's group developed the concept of biology-oriented synthesis (BIOS), which integrates computational and synthetic tools to design and synthesize bioactive simplified NP analogues by mapping both the biologically relevant chemical space and the target protein space[76]. The development of highly efficient and practical synthetic methods is the heart of BIOS. Waldmann and coworkers[77] reported a series of novel BIOS-inspired

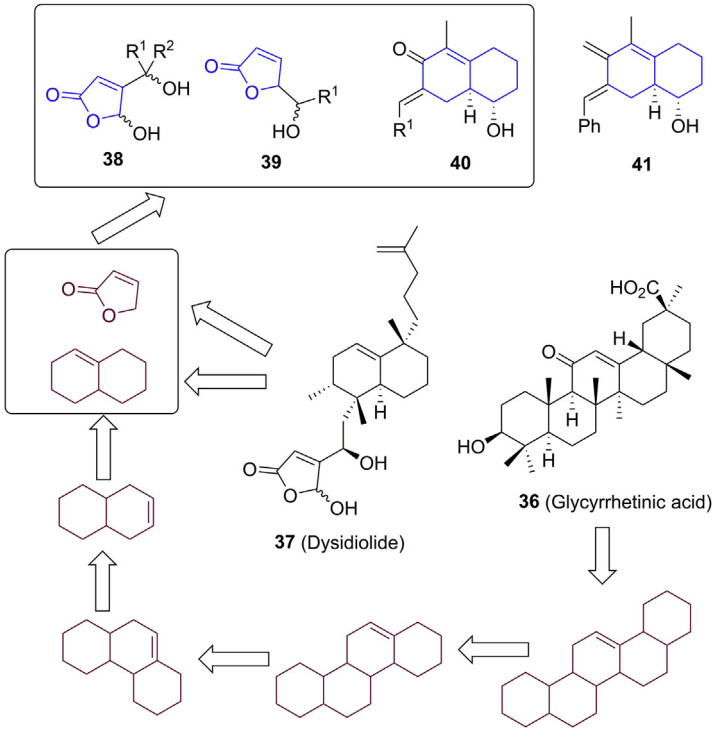


**Figure 7** A structural classification of natural product (SCONP) scaffold tree generated from glycyrrhetinic acid and dysidiolide and compound libraries inspired by these simplified scaffolds.

synthetic methods and constructed new compound libraries for chemical biology and medicinal chemistry studies. Phenotypic or target-based screenings of BIOS compound libraries in combination with target identification have successfully yielded several novel classes of bioactive compounds[78]. Using biologically prevalidated NPs as starting points and using a hierarchically arranged scaffold tree for guidance, a typical BIOS library contains only 200 to 500 compounds and results in relatively high hit rates (approximately 0.5%−1.5%)[77], showing the promise of applying BIOS in chemical biology and drug discovery.

The 3,3′-pyrrolidinyl-spirooxindole scaffold is responsible for a wide variety of biological activities[79]. For example, spirotryprostatin B (**42**, Fig. 8) is an inhibitor of tubulin polymerization and arrests the cell cycle at the G2/M phase. Waldmann's group constructed an NP-inspired 3,3′-pyrrolidinyl spirooxindole library (**43**) by a highly enantioselective, Lewis acid-catalyzed 1,3-dipolar cycloaddition reaction[80]. Cellular evaluations revealed that compound **(−)-44** interfered with microtubule polymerization rather than inhibiting p53-MDM2 interactions[80].

Mono-, bi-, and tricyclic oxepanes are biologically relevant scaffolds embedded in a number of NPs (*e.g.,* sodwanone S, **45**, Fig. 9) that show various bioactivities[81]. Waldmann and coworkers[82] developed new one-pot cascade reactions for the synthesis of NP-inspired oxepane libraries (**46** and **47**). Among the prepared compounds, novel WNT-signaling modulators were identified by a reporter gene assay. Oxepane **48** was the most active compound with an $ED_{50}$ value of 1.8 μmol/L. Moreover, its simplified analogue, **49**, retained this activity ($ED_{50}$ = 9.9 μmol/L). Target identification using a chemical proteomics approach indicated that compound **48** reversibly bound to van-Gogh-like receptor protein 1 (VANGL1)[82].

Polycyclic indole alkaloids (*e.g.,* vinblastine, **50**, Fig. 10) are a rich source of mitosis-targeting agents[83]. Dückert et al[84]. developed highly efficient cascade reactions to synthesize NP-inspired indoloquinolizines (**51**). Cellular screening in combination with target identification revealed that compound (*R*)**-52** was a unique dual modulator of centrosome-associated protein nucleophosmin (NPM) and nuclear export receptor CRM1[84]. The dual targeting of NPM and CRM1 in cancer cells led to the impairment of centrosome and spindle integrity, providing a new platform for novel antitumor drug discovery.

## 3. Structural simplification of bioactive small molecules

### 3.1. *Structural simplification by reducing the number of rings*

#### 3.1.1. *Discovery of dabrafenib through structural simplification and optimization*

B-RAF, a member of the protein kinase RAF family, plays a central role in the MAPK signaling pathway[85]. The most common mutation, observed in 80%−90% of *B-RAF* mutant cancers, is the *B-RAF* V600E mutation, which destroys the kinase activity and then causes cell carcinogenesis[86,87]. Therefore, inhibitors of $B\text{-}RAF^{V600E}$ kinase activity offer a novel targeted approach for the treatment of *B-RAF* V600E-driven cancers, particularly melanoma and colon cancer[88]. Compound **53** (Fig. 11A), a B-RAF inhibitor identified by GSK oncology-directed kinase programs, features an imidazopyridine core and a large hydrophobic benzamide headgroup[89]. Although this compound potently inhibits $B\text{-}RAF^{V600E}$ ($IC_{50}$ = 9 nmol/L), it showed poor antiproliferative activity in cell-based assays against the $B\text{-}RAF^{V600E}$ SKMEL28 melanoma cell line ($EC_{50}$ = 5.32 μmol/L, Table 1[89,90]). Compound **53** has a molecular weight of 605 with a low LE value (0.24). Therefore, modest simplification of compound **53** was required to increase its LE value and improve its cellular activity.

The process for lead optimization and simplification is shown in Fig. 11A[89,90]. First, headgroup SAR was explored by preparing a set of analogues in which the amide linker was replaced by a series of other groups such as ureas and sulfonamides[89]. Biological assays revealed that sulfonamide-containing analogue **54** showed a substantial improvement in cellular potency. Replacing the imidazopyridine core with a thiazole afforded 2-isopropylthiazole analogue **55**, which displayed an increased LE value (0.26). Further replacement of the *N*-methyl-tetrahydroisoquinoline tail of **55** with an *N*-acetylpiperazinylpyridine afforded compound **56**, which showed substantial improvements in enzyme ($IC_{50}$ = 3.6 nmol/L) and cellular activity (pERK $EC_{50}$ = 7 nmol/L, SKMEL28 $EC_{50}$ = 24 nmol/L, Table 1)[89]. However, it had poor metabolic stability, as it was easily metabolized by rat liver microsomes (CL = 20 mL/min/g). Using the headgroup of **53**, 2,6-difluorinated analogue **57** showed improved metabolic stability (CL = 7 mL/min/g)[89]. Subsequent acetylpiperazine/morpholine replacement had little effect on the cellular potency; however, **58** did present improved activity toward $B\text{-}RAF^{V600E}$ ($IC_{50}$ = 0.5 nmol/L). Pharmacokinetic studies revealed that compound **58** showed good oral availability and clearance in rats, but poor pharmacokinetics were observed in dogs and monkeys[89].

After structural analysis, the MW of compound **58** was 667, which is too large for an oral drug. Therefore, structural simplification involving replacing the pyridinylmorpholine with simpler alkyl groups was performed[90]. For example, ethylmethylsulfone analogue **59** showed excellent B-RAF V600E inhibitory activity ($IC_{50}$ = 0.3 nmol/L, Table 1). Pharmacokinetic studies revealed that *N*-dealkylated compound **60** was the major metabolite of **59**, but it was less active than the parent compound ($IC_{50}$ = 40 nmol/L, Table 1). The isopropyl group was replaced with a *tert*-butyl group in an attempt to further improve the metabolic stability

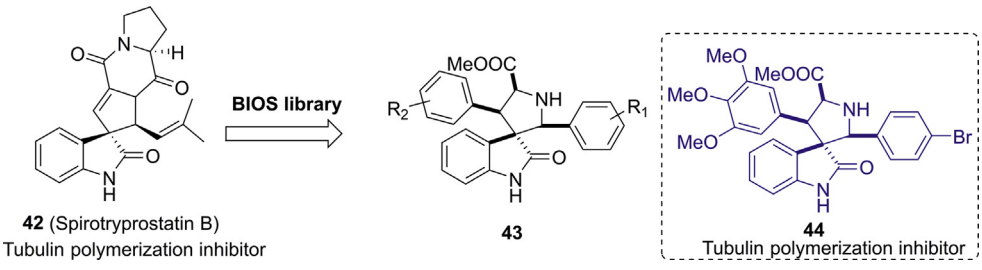


**Figure 8** Biology–oriented synthesis (BIOS) library inspired by spirotryprostatin B and bioactive simplified analogues.

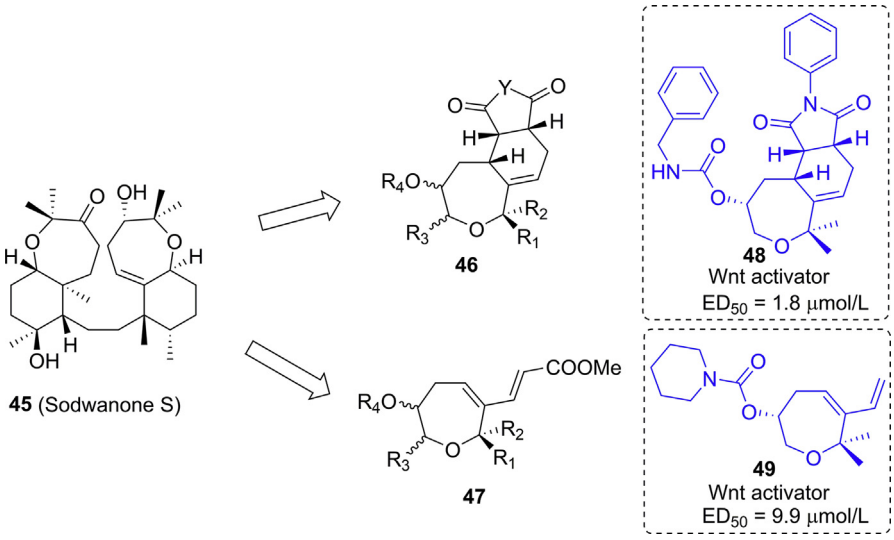


**Figure 9** BIOS library inspired by sodwanone S and bioactive simplified analogues.

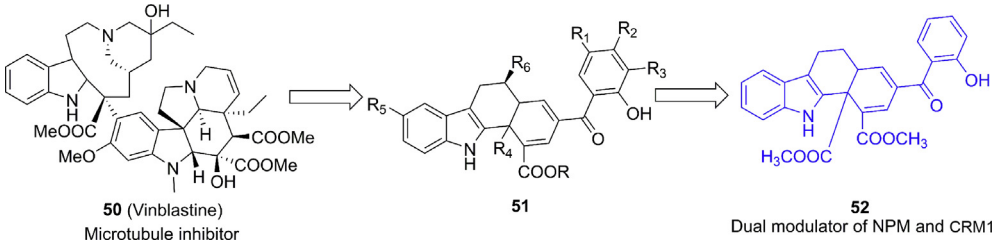


**Figure 10** BIOS library inspired by vinblastine and bioactive simplified analogues.

and bioavailability[90]. For example, compound **61** had good *in vitro* and *in vivo* activities. Finally, removing the ethylmethylsulfone group of the tail and optimizing the substituents at each site afforded compound **62** (dabrafenib). It displayed excellent inhibitory activity for B-RAF$^{V600E}$ ($IC_{50}$ = 0.7 nmol/L, Table 1) and had favorable pharmacological, pharmacokinetic and physicochemical properties. Compared to lead compound **53** (MW = 605, LE = 0.24), the MW of dabrafenib was reduced to 519, and the LE value was increased to 0.33 (Table 1). The co-crystal structure of dabrafenib with B-RAF$^{V600E}$ (PDB code: 4XV2) revealed the aminopyrimidine and sulfamide groups of dabrafenib formed several hydrogen bonds with Cys532, Lys483, Phe595 and Asp594 (Fig. 11B)[91]. The difluorophenyl and *t*-butyl groups formed hydrophobic interactions with surrounding hydrophobic residues (Fig. 11B). Dabrafenib, developed by GSK, was approved by the FDA in 2013 for the treatment of unresectable or metastatic malignant melanomas with B-RAF V600E or V600K mutations[92].

### 3.1.2. *Discovery of tofacitinib through structural simplification and optimization*

The Janus tyrosine kinases (JAKs) include four subtypes, JAK1, JAK2, JAK3 and Tyk2[93]. Among them, JAK3 is an important drug target for the treatment of autoimmune diseases, and its inhibitors can regulate or suppress immune function. JAK1 is broadly expressed, and the inhibition of JAK1 is anticipated to play a role in cellular potency either additively or synergistically with JAK3 due to the manner in which these enzymes operate together at the IL-2 receptor[94]. JAK2 plays an essential role in hematopoiesis, including in *epo* receptor signaling and red blood cell homeostasis[95], and its inhibitors could lead to undesired effects such as anemia[94]. Therefore, the development of JAK3 inhibitors should improve the inhibitory selectivity for JAK2 and result in good inhibitory activity for JAK1 while at the same time producing a synergistic effect. Researchers at Pfizer performed a high-throughput screening and identified selective JAK3 inhibitor **63** (Fig. 12). It showed good inhibitory activity for JAK3 ($IC_{50}$ = 210 nmol/L), and it was 45-fold less potent against JAK2 and inactive against JAK1 ($IC_{50}$ > 10 μmol/L, Table 2)[94,96]. A cell-based assay (IL-2-induced proliferation of human T-cell blasts) revealed that compound **63** only moderately inhibited cellular activity ($IC_{50}$ = 3200 nmol/L), meaning there was substantial room for improvement. In addition, the half-life of compound **63** in human liver microsome (HLM) was short (15 min). Therefore, structural optimizations focused on improving the JAK3 inhibitory activity and selectivity as well as its metabolic stability[94].

Compound **63** contains five rings, and the first step in structural optimization was to reduce the number of rings and MW, leaving room for subsequent optimization. Flanagan et al.[94] replaced the carbazole group with *N*-methyl-cycloalkyl groups, and the resulting analogues (**64**) demonstrated greater potency against JAK1, while the JAK3 inhibitory activity was retained. Moreover,

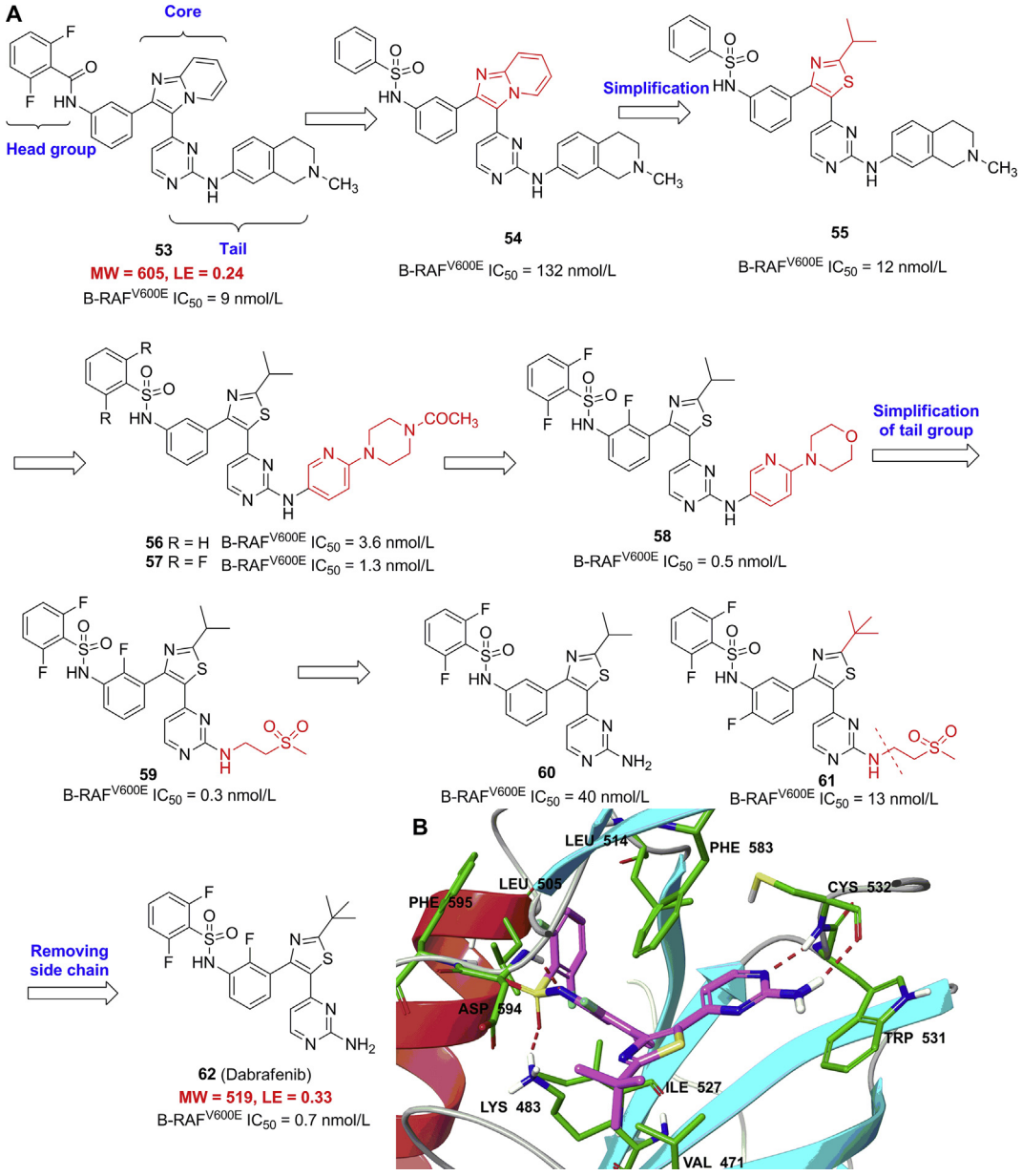


**Figure 11** Structural simplification process to discover dabrafenib (A) and the binding mode of dabrafenib with B-RAF$^{V600E}$ (B, PDB code: 4XV2).

**Table 1** Enzyme potencies ($IC_{50}$, nmol/L), cell potencies ($EC_{50}$, nmol/L) and ligand efficiency (LE) of B-RAF inhibitors.

| Compd. | B-RAF$^{V600E}$ ($IC_{50}$) | pERK ($EC_{50}$) | SKMEL28 ($EC_{50}$) | LE |
|---|---|---|---|---|
| **53** | 9 | >10,000 | 5316 | 0.24 |
| **54** | 132 | 99 | 1.11 | 0.22 |
| **55** | 12 | 52 | 287 | 0.26 |
| **56** | 3.6 | 7 | 24 | 0.24 |
| **57** | 1.3 | 10 | 12 | 0.25 |
| **58** | 0.5 | 11 | 8 | 0.28 |
| **59** | 0.3 | 7 | 10 | 0.28 |
| **60** | 40 | 78 | 61 | 0.29 |
| **61** | 13 | 11 | 87 | 0.26 |
| **62** | 0.7 | 4 | 3 | 0.33 |

these analogues showed improved whole−cell activity over that of the lead compound (**63**). For example, *N*-methyl-cyclohexyl analogue **65** was a highly active JAK3 ($IC_{50}$ = 20 nmol/L) and T-cell ($IC_{50}$ = 340 nmol/L) inhibitor, but its metabolic stability was still poor ($t_{1/2}$ = 18 min, Table 2). Subsequently, natural carvone (**66**) was used as the chiral source to replace the 2′,5′-dimethyl cyclohexane moiety of compound **65**. A kinase assay revealed that compound **69** was the most potent isomer (JAK3 $IC_{50}$ = 2 nmol/L; cellular $IC_{50}$ = 50 nmol/L, Table 2). However, the PK profiles, such as its microsomal stability (HLM $t_{1/2}$ = 14 min), aqueous solubility (1.3 μg/mL) and rat bioavailability (~7%) of compound **69**, were unfavorable[94]. To address this problem, the carvone moiety was replaced with piperidinyl amide groups. After incorporation of a nitrogen atom, the aqueous solubility was significantly improved, and one chiral center was eliminated, which facilitated analogue synthesis (**70**, Fig. 12).

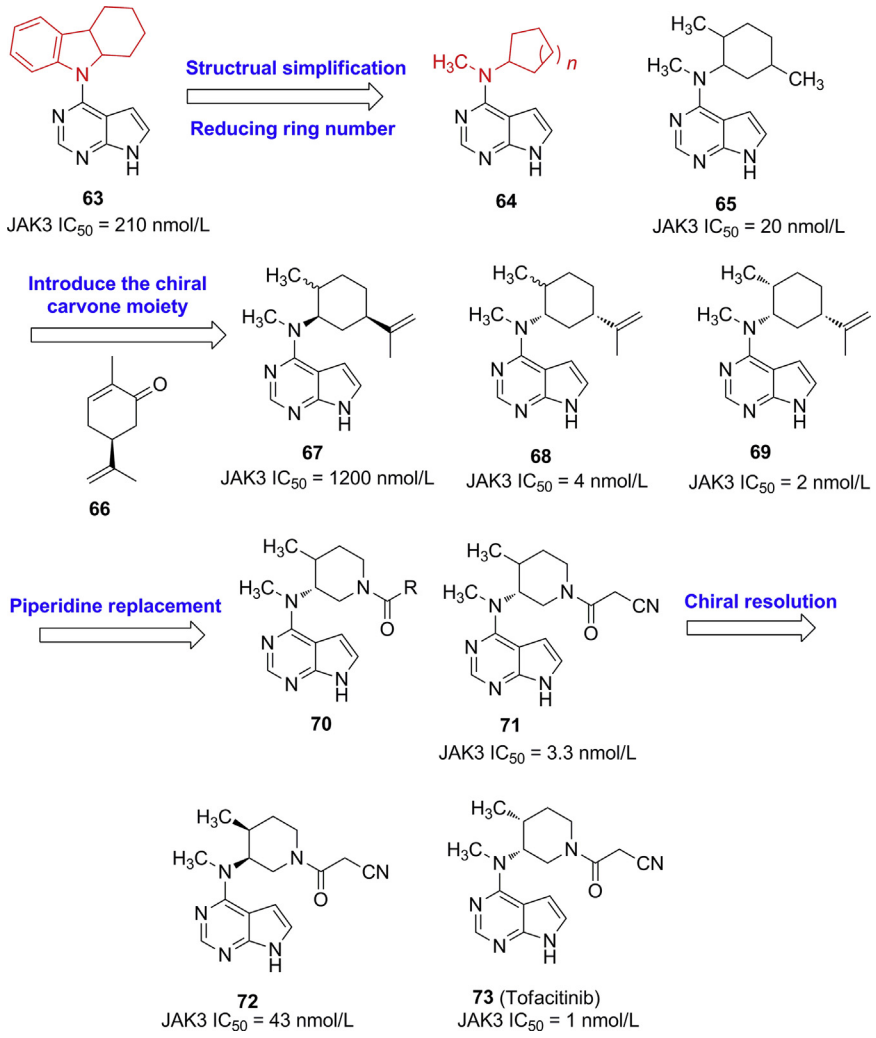


**Figure 12** Discovery of tofacitinib through structural simplification and optimization.

Among the prepared analogues, compound **71** displayed the highest potency (JAK3 $IC_{50}$ = 3.3 nmol/L; cellular $IC_{50}$ = 40 nmol/L, $t_{1/2}$>100 min) and favorable metabolic stability. Further evaluation of its enantiomers revealed that (3*R*,4*R*) isomer **73** had an $IC_{50}$ value of 1 nmol/L against JAK3, making it approximately 40-fold more potent than (3*S*,4*S*) isomer **72**. In addition, compound **73** had desirable characteristics, including good solubility (>4 mg/mL in water), metabolic stability (HLM $t_{1/2}$>120 min) and oral bioavailability (78% in dogs). Therefore, compound **73** (tofacitinib) was approved by the FDA in 2012 as the first-in-class oral JAK inhibitor for the treatment of rheumatoid arthritis.

**Table 2** Biological activities and metabolic stabilities of selected JAK inhibitors.

| Compd. | JAK3 (nmol/L) | JAK2/ JAK3 | JAK1 (nmol/L) | Cell $IC_{50}$ (nmol/L)[a] | HLM $t_{1/2}$ (min) |
|---|---|---|---|---|---|
| **63** | 210 | 45 | >10,000 | 3200 | 15 |
| **65** | 20 | – | – | 340 | 18 |
| **67** | 1200 | – | – | 8900 | – |
| **68** | 4 | – | – | 90 | – |
| **69** | 2 | – | – | 50 | 14 |
| **71** | 3.3 | 20 | 110 | 40 | >100 |
| **72** | 43 | – | – | 580 | – |
| **73** | 1 | 20 | – | 11 | >120 |

–Not available.
[a]Determined using an IL-2-induced T-cell blast proliferation assay.

### 3.1.3. *Structural simplification of GlyT1 inhibitors*

Recent studies have indicated that selective glycine transport 1 (GlyT1) inhibitors have the potential to alleviate symptoms of schizophrenia[97,98]. In their search for novel selective GlyT1 inhibitors, scientists at Roche performed a high-throughput screening and found several hits[99]. Compound **74** (Fig. 13) showed potent inhibitory activity against GlyT1 ($EC_{50}$ = 154 nmol/L). However, the 5-phenyl-benzodiazepine-2-one scaffold could cause off-target toxicities[99]. Therefore, the potential liability of the benzodiazepine moiety and relatively high MW (506) prompted the design of structurally simpler derivatives. Based on the SAR indicating that the benzodiazepinone moiety was not essential for the GlyT1 inhibitory activity, Jolidon et al.[99]

replaced it with a simpler diarylmethylamine scaffold, which also mimicked the key interactions with the target. Simplified analogue **75** (Fig. 13) displayed more potent GlyT1 inhibitory activity ($EC_{50}$ = 16 nmol/L) than was seen with lead compound **74**. Moreover, **73** showed excellent metabolic stability.

*3.1.4. Structural simplification of CGRP receptor antagonists*

Calcitonin gene-related peptide (CGRP) exhibits potent vasodilation activity and is involved in the pathogenesis of migraine[100]. Recent studies revealed that CGRP antagonists could be efficacious and well tolerated in the migraine treatment[101,102]. Two small-molecule CGRP receptor antagonists, olcegepant and telcagepant, effectively normalized circulating CGRP levels with concomitant pain relief[101,103]. Bell et al[102]. reported a novel class of CGRP inhibitors with high potency (**76**, $K_i$ = 0.13 nmol/L, Fig. 14) and good pharmacokinetics. However, synthetic difficulties associated with the structural complexity of compound **76** hampered the rapid exploration of SAR. To discover novel CGRP receptor antagonists, Selnick et al.[102] performed a systematic step-by-step simplification of **76**. First, the pyridine substructure of **76** was replaced by an amide, which had little impact on the binding affinity, while greatly simplifying the synthetic route as a straightforward amide coupling could then be used. The replacement of the azaoxindole group in **76** by hydantoin (compound **77**) decreased the binding affinity by approximately 10-fold but allowed the use of more readily available starting materials. Deletion of the 6-membered lactam in **76** simplified the tricyclic structure to a bicyclic structure. Further scission of the remaining 5-membered lactam afforded compounds **78** and **79**, which facilitated additional modifications. Compound **79**, which possessed a benzyl group ($n$ = 1), displayed more potent CGRP binding affinity ($K_i$ = 10 nmol/L) than compound **78** ($K_i$ = 140 nmol/L). The hydroxyl group of **79** was then removed, and *S*-isomer **80** displayed an improved CGRP binding affinity ($K_i$ = 1.9 nmol/L). However, analogue **80** also showed a submicromolar binding affinity to the closely related adrenomedullin-2 receptor (AM2, $K_i$ = 720 nmol/L), which could cause off-target toxicities. Therefore, further modifications were focused on improving the enzymatic selectivity. By optimizing the substituents at the benzylic position and on the benzyl group of **80**, analogue **81**, with a 3,5-difluorophenyl substituent, displayed the best CGRP inhibitory activity ($K_i$ = 0.26 nmol/L) and enzymatic selectivity (AM2 $K_i$ = 1400 nmol/L, $SI_{AM2/CGRP}$>5000). Straightforward application of Ellman sulfinimide synthetic methodologies afforded lactams **82** ($K_i$ = 0.23 nmol/L) and **83** ($K_i$ = 0.48 nmol/L), and their CGRP antagonistic activities revealed that the methyl group at the benzylic position was not beneficial to the binding affinity. Starting from **82**, the azaoxindole group of **76** was reintroduced to afford analogue **84**, which displayed the best CGRP inhibitory activity ($K_i$ = 0.035 nmol/L) and excellent selectivity ($SI_{AM2/CGRP}$ = 4600). Compared with lead compound **76**, simplified analogue **84** is easier to synthesize and possesses improved potency.

*3.1.5. Structural simplification of nootropic agents*

4-Substituted 1,4-diazabicyclo[4.3.0]nonan-9-ones are extremely potent nootropic agents according to a mouse passive avoidance test[104]. The most active derivative, DM232 (**85**, Fig. 15), prevented amnesia at doses as low as 0.001 mg/kg sc[104]. Gualtieri et al.[105] simplified the structure of DM232 *via* the scission of the 5-membered lactam ring to afford 4-substituted 1-acylpiperazines (**86**). The simplified analogues maintained the high nootropic activity of the parent compound, indicating that an *N*-acylpiperazine group could mimic the 2-pyrrolidinone ring of DM232. An *in vivo* mouse passive avoidance test revealed that DM235 (**87**, Fig. 15) displayed comparable potency (active at a dose of 0.001 mg/kg, sc) to that of lead compound DM232.

*3.1.6. Structural simplification of $hA_3$ AR antagonist*

Human A3 adenosine receptor ($hA_3$ AR) is a member of the G-protein-coupled receptor (GPCR) family that is involved in modulating various physiopathological conditions. Selective $hA_3$ AR antagonists were found to be beneficial in treating inflammatory, asthmatic and ischemic conditions. Moreover, the A3 receptor is overexpressed in several tumor cell lines, making it a potential target for cancer therapy. Tricyclic 2-aryl-1,2,4-triazolo[4,3-*a*]quinoxalin-1-one derivatives, either 4-amino- or 4-oxo-substituted derivatives (represented by **88** and **91**, Fig. 16), displayed high affinities and selectivities for $hA_3$ AR[106]. To shorten the synthetic route and improve the pharmacokinetic profile, Moro et al.[107] performed structural simplification studies to afford synthetically more tractable 2-amino/2-oxoquinazoline-4-carboxamido analogues. For example, starting from tricyclic compound **88**, 2-oxoquinazoline-4-carboxamido analogues **89** were obtained *via* opening the C ring. Their planar conformations were similar to that of compound **88** because of the presence of an intramolecular hydrogen bond. Among these analogues, **90** displayed a binding affinity toward $hA_3$ AR ($K_i$ = 19.5 nmol/L) comparable to that of lead compound **88** ($K_i$ = 16 nmol/L). Notably, these simplified analogues displayed significantly enhanced solubility compared to their tricyclic parent compound. However, further removing the planar aromatic ring (A ring) afforded 2-aminopyrimidine-4-carboxyamides (**92**), which were completely inactive toward $hA_3$ AR.

Moro and coworkers identified the 2-phenylphthalazin-1(2*H*)-one ring system (such as that in **93**) as a simplified scaffold for the design of novel $hA_3$ AR antagonists[108]. Among the prepared analogues, **94** was a highly potent and selective $hA_3$ AR antagonist ($K_i$ = 0.776 nmol/L; $hA_1/hA_3$ and $hA_{2A}/hA_3$>12,000). The same group also used a scaffold simplification strategy to improve the selectivity of the pyrazolo-[3,4-*c*]quinolin-4-one $hA_3$ AR antagonists (**95**)[109]. After removing the A ring, the 2-arylpyrazolo[4,3-*d*]pyrimidin-7-one analogues (**96**) displayed high $hA_3$ AR affinities

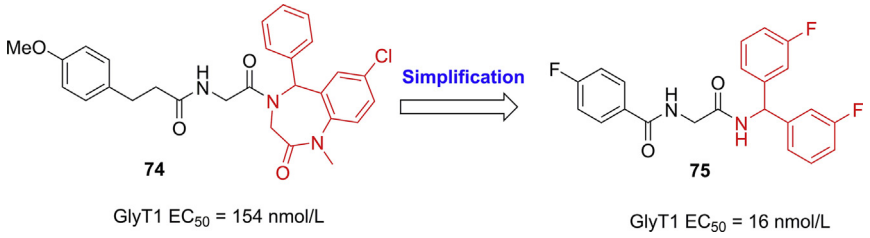


**Figure 13** Structural simplification of GlyT1 inhibitors.

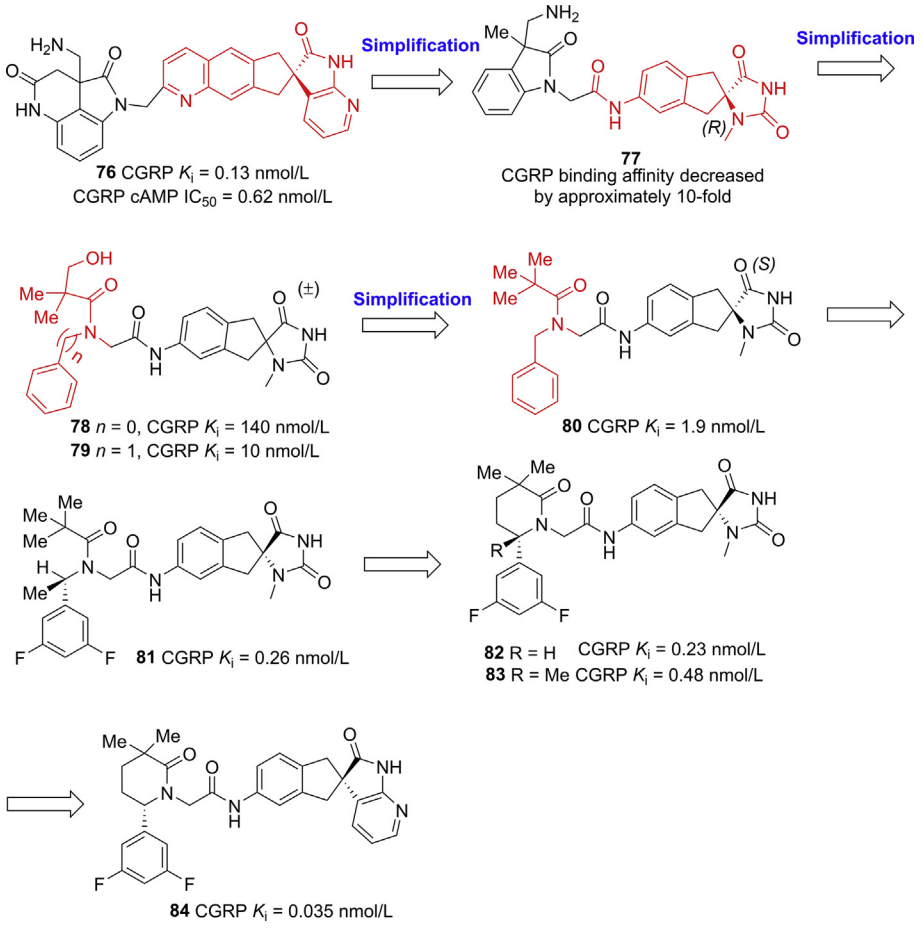


**Figure 14** Structural simplification of CGRP receptor antagonists.

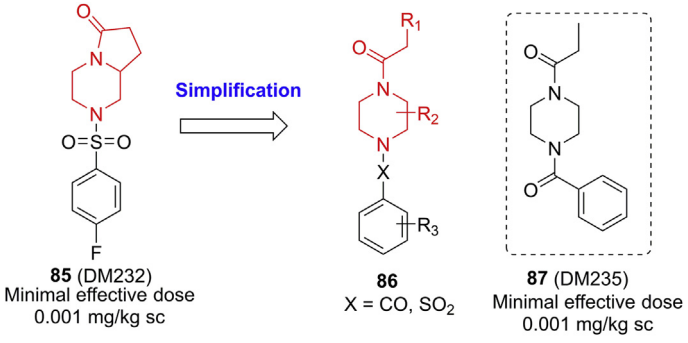


**Figure 15** Structural simplification of nootropic agents.

in the low nanomolar range ($K_i$ range: 1.2−72 nmol/L)[110]. Among these compounds, **97** displayed the best $hA_3$ AR affinity with a $K_i$ value of 1.2 nmol/L, and it was completely inactive toward $hA_1$, $hA_{2A}$, and $hA_{2B}$ ARs.

Pastorin et al.[111] reported that pyrazolo-triazolo-pyrimidine derivative **98** is a potent and highly selective $hA_3$ AR antagonist ($hA_3$ AR $K_i$ = 0.108 nmol/L; $hA_1/hA_3$ = 5200; $hA_{2A}/hA_3$ = 7200). However, the tricyclic compound has a high molecular weight and a complex scaffold, leading to unfavorable drug-like properties, such as poor aqueous solubility and synthetic difficulty. To address these drawbacks, the same group simplified the tricyclic scaffold by removing the A ring to afford novel bicyclic pyrazolo[3,4-*d*]pyrimidine derivatives (**99**)[112]. However, compound **100** ($K_i$ = 0.9 μmol/L) showed lower affinity than its parent compound. Nonetheless, the authors considered it a good starting point for developing more potent $hA_3$ AR antagonists.

### *3.1.7. Structural simplification of cruzain inhibitors*

Cruzain is the major cysteine protease of *Trypanosoma cruzi*, which is an attractive target for antiparasitic agents due to its

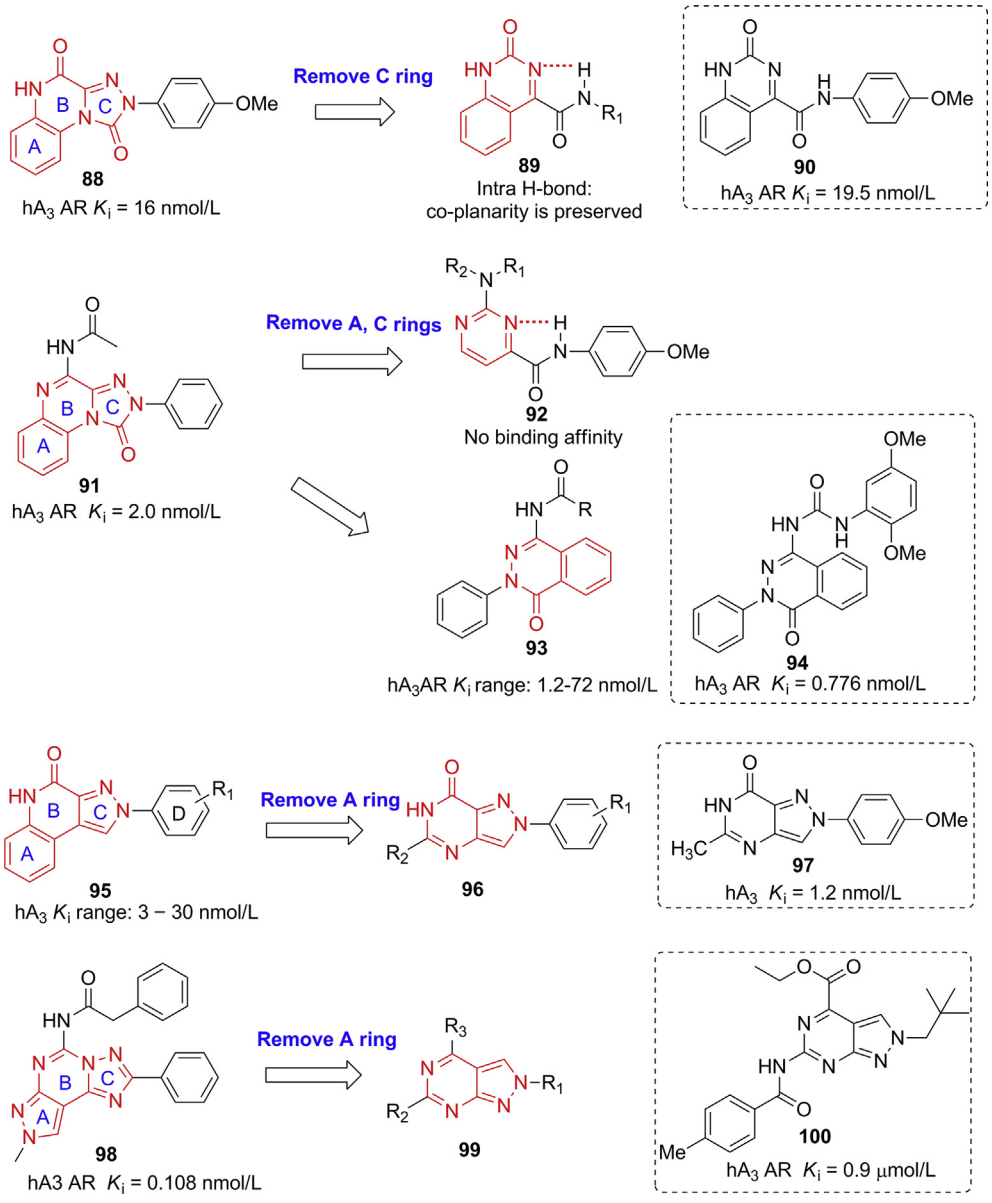


**Figure 16** Structural simplification of $hA_3$ AR antagonist.

essential functions in parasites[113]. Through a combination of docking studies and high-throughput screening, Shoichet et al.[114] identified indole-pyrimidine **101**, which showed good cruzain inhibitory activity ($K_i$ = 2.0 μmol/L; $IC_{50}$ = 2.5 μmol/L) and represents a promising lead structure for the development of antiparasitic agents. Oliveira et al.[115] simplified the scaffold of compound **101** (Fig. 17) by using mono- or bicyclic heterocycles such as quinoline (**102**), indole (**103**), aniline (**104**), pyrrole (**105**) and pyrimidine (**106**). A biological assay revealed that compound **107** displayed the best cruzain inhibitory activity ($IC_{50}$ = 15 μmol/L) with moderate cellular potency against *T. cruzi* ($IC_{50}$ = 67.7 μmol/L). Although further simplified pyrimidine derivative **108** showed improved activity against *T. cruzi* ($IC_{50}$ = 3.1 μmol/L) with excellent selectivity (SI = 128), it was completely inactive against cruzain, indicating that it might have a different mechanism of action.

### *3.2. Structural simplification by reducing the number of chiral centers*

#### *3.2.1. Structural simplification of CDC7 kinase inhibitors*

CDC7 kinase is an essential protein that promotes DNA replication in eukaryotic organisms. Inhibition of CDC7 causes selective tumor-cell death in a p53-independent manner, suggesting small-molecule CDC7 inhibitors could be developed as anticancer agents[116,117]. A series of pyrrolopyridinone derivatives, represented by compound **109** (Fig. 18), were shown to be potent and selective CDC7 kinase inhibitors[118]. The co-crystal structure of compound **109** with CDC7 kinase (PDB code: 4F9B) revealed the pyridine and lactam moieties of **109** formed three hydrogen bonds with residues Leu137, Lys90 and Asp196 (Fig. 18B)[119]. Further SAR studies led to the discovery of compound **110**, which showed excellent CDC7 inhibitory activity ($IC_{50}$ = 0.002 μmol/L) and

acceptable selectivity against a panel of unrelated kinases[120]. Moreover, it displayed good potency in a cell proliferation assay (A2780 ovarian carcinoma, $IC_{50}$ = 0.5 μmol/L). Similar to compound **109**, molecular docking simulation revealed that compound **110** formed hydrogen bonding interaction with residues Leu137, Lys90 and Asp196 (Fig. 18C). Moreover, the aminopyrimidine group formed an additional hydrogen bond with Pro135 (Fig. 18C). However, further evaluations indicated that compound **110** had unfavorable pharmacokinetic behavior in animal species (*e.g.*, rapid clearance from plasma). To improve the PK properties, Menichincheri et al.[121] simplified the scaffold by opening the lactam ring to afford 5-heteroaryl-3-carboxamido-2-substituted pyrrole derivatives. In addition, the elimination of the stereogenic center also facilitated chemical synthesis and SAR investigations. Representative analogue **111** (Fig. 18) displayed excellent inhibitory activity against CDC7 ($IC_{50}$ = 0.009 μmol/L); however, it was only moderately active in an A2780 cellular assay ($IC_{50}$ = 2.0 μmol/L). Further modifications were focused on the replacement of ring A and central core B with various heterocycles (**112**). Several of the resulting analogues displayed good CDC7 kinase inhibitory activities, *in vitro* antiproliferative activities and favorable PK properties. In particular, compound **113** was orally active and displayed excellent *in vivo* antitumor potency against A2780 ovarian carcinoma (tumor growth inhibition, TGI>90%), HCT-116 (TGI = 68%) and COLO-205 (max TGI = 41%) colorectal cancer xenograft models. Similar to compound **110**, compound **113** also formed several hydrogen bonds with Leu137, Lys90, Asp196 and Pro135 (Fig. 18D).

### 3.2.2. *Structural simplification of ATP synthase inhibitors*

In 2012, bedaquiline (**114**, Fig. 19), which blocks the proton pump for ATP synthase of mycobacteria, was approved for the treatment of multidrug-resistant tuberculosis (MDR-TB)[122,123]. However, bedaquiline has two adjacent chiral centers, making its chemical synthesis laborious and costly. Therefore, reducing the structural complexity of bedaquiline while retaining its potent antitubercular activity is of great importance. Yin et al.[124] systematically simplified the structure of bedaquiline by removing the two adjacent chiral centers, which greatly streamlined the synthetic process. Analogue **115** displayed potent *in vitro* antitubercular activities against both the drug-sensitive *mycobacterium tuberculosis* (*M. tuberculosis*) strain H37Rv (MIC = 0.43 μg/mL) and drug-resistant strain 12153 (MIC = 0.48 μg/mL).

### 3.2.3. *Structural simplification of LeuRS-targeted mTORC1 inhibitors*

Recent studies indicated that leucyl-tRNA synthetase (LeuRS) may act as a leucine sensor for the mammalian target of rapamycin complex 1 (mTORC1) pathway, potentially providing an alternative strategy for overcoming rapamycin resistance in cancer treatments[125,126]. In 2016, Lee et al.[127] reported leucyladenylate sulfamate derivative **116** as a novel LeuRS-targeted mTORC1 inhibitor (Fig. 20). Compound **116** selectively inhibited LeuRS-mediated mTORC1 activation and exerted specific cytotoxicity against colon cancer cells with hyperactive mTORC1. However, its high polarity hindered further preclinical development as it resulted in synthetic difficulties and poor bioavailability. To resolve these obstacles, Lee et al.[128] performed further structural simplifications by replacing the adenylate group of leucyladenylate sulfamate with an *N*-(3,4-dimethoxybenzyl) benzenesulfonamide group (red part, Fig. 20). Simplified analogues **117**, which were less polar and had fewer asymmetric centers, had more favorable physicochemical properties. Biological assays revealed that 3,4-dimethoxybenzyl analogues **117** generally showed good activities. For example, compound **118** and its constrained analogue **119** demonstrated micromolar inhibitory activities against six types of cancer cells (Table 3[127,128]), and their activities were comparable to those of lead compound **116**. They effectively inhibited S6K phosphorylation in a dose-dependent manner without affecting the catalytic leucylation activity of LeuRS.

## 3.3. *Structural simplification by structure-based design*

### 3.3.1. *Structural simplification of aminoacyl-tRNA synthetases inhibitors*

Aminoacyl-tRNA synthetases (aaRSs) are a class of enzymes that have been validated as antimicrobial targets[129–132]. Most aaRS inhibitors are targeted at their synthetic active site by mimicking the endogenous substrate aminoacyl-AMP (aa-AMP) or its stable analogue aminoacylsulfa-moyladenosine (aa-AMS). Although potent inhibitors have been discovered, they generally

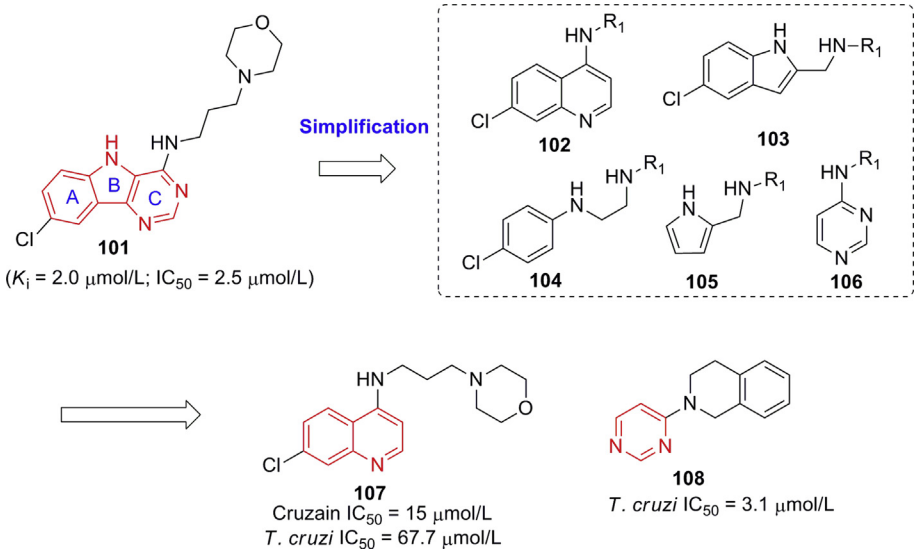


**Figure 17** Structural simplification of cruzain inhibitors.

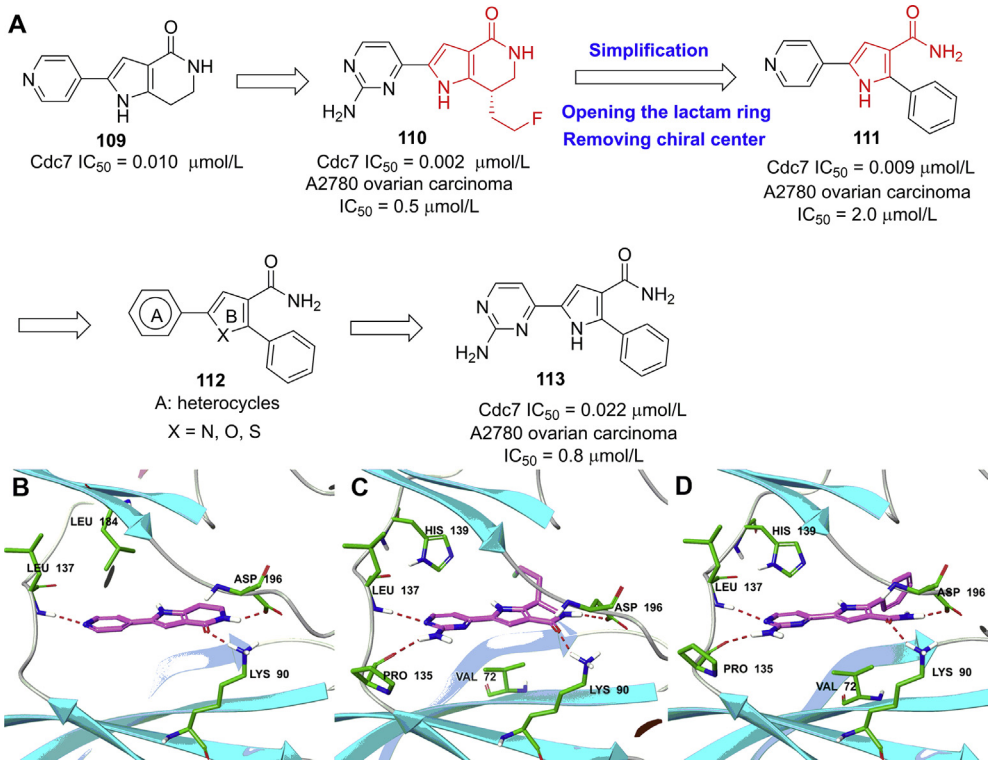


**Figure 18** Structural simplification of CDC7 kinase inhibitors (A) and the binding modes of compounds **109** (B, PDB code: 4F9B), **110** (C) and **113** (D) with CDC7 kinase.

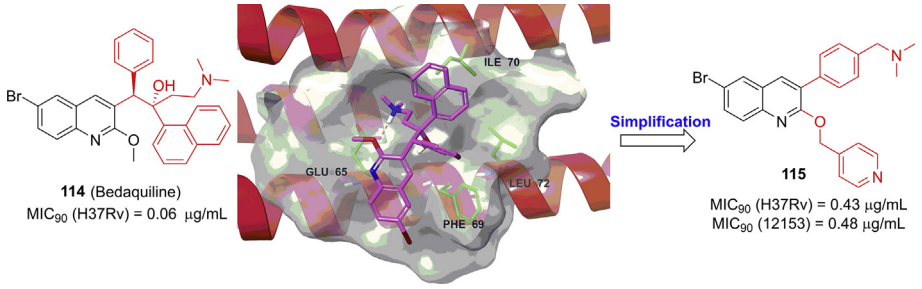


**Figure 19** Structural simplification of ATP synthase inhibitors and binding mode of bedaquiline with mycobacterial ATP synthase rotor ring (PDB code: 4V1F).

lack both selectivity and antibacterial potency. To address these issues, Teng et al.[133] designed and synthesized threonyl-tRNA synthetase (ThrRS) inhibitors by structure-based design (Fig. 21). The co−crystal structure of Thr-AMS (**120**) with *Escherichia coli* ThrRS (PDB code: 1KOG)[134] revealed the adenine and acylsulfonamide moieties of Thr-AMS formed a tight hydrogen bonding network with surrounding residues including Val376, Glu365, Arg363, Gln381 and Gln484 (Fig. 21B). Moreover, the amino–alcohol groups chelated the $Zn^{2+}$ in the active site of *E. coli* ThrRS (Fig. 21B). First, they simplified Thr-AMS by replacing the polar adenosine moiety with a 4-phenoxyphenyl moiety while retaining the acylsulfonamide moiety (**121**). These changes resulted in a loss of potency due to the absence of the hydrogen bonding network involving adenosine (Fig. 21C). To restore the hydrogen bonding interactions, the distal phenoxyl group was replaced with heterocyclic fragments, such as quinazoline, isoquinoline, aminopyrimidine and pyrrolopyrimidine. Several analogues displayed selective inhibitory activities against *E. coli* ThrRS and moderate antibacterial activity against *H. influenzae* at nanomolar concentrations. Among the indazole derivatives, **122** displayed the best *E. coli* and human ThrRS selectivity radio (*E. coli* ThrRS $K_i$ = 0.18 μmol/L, human ThrRS $K_i$>50 μmol/L). The co-crystal structure of compound **122** with *E. coli* ThrRS (PDB code: 4HWR)[133] revealed the indazole moiety formed two hydrogen bonds with residue Val376. Similar to Thr-AMS, the acylsulfonamide side chain of compound **122** chelated the $Zn^{2+}$ in the active site and formed a hydrogen bonding network with surrounding residues including Lys465, Arg363, Gln381 and Gln484 (Fig. 21D).

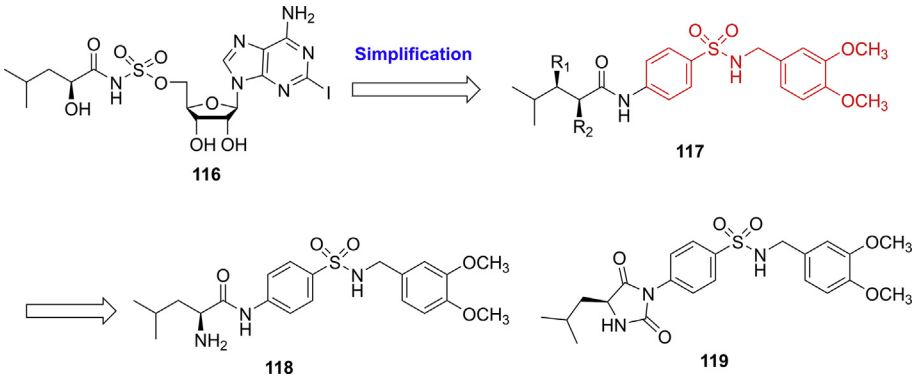


**Figure 20** Structural simplification of LeuRS-targeted mTORC1 inhibitors.

**Table 3** *In vitro* antitumor activity of simplified LeuRS-targeted mTORC1 inhibitors ($IC_{50}$, μmol/L).[a]

| Compd. | A549 | HCT116 | K562 | MDA-MB-231 | SK-HEP-1 | SNU638 | MRC5 |
|---|---|---|---|---|---|---|---|
| **116** | 1.75 | 0.54 | 1.06 | 12.6 | 5.63 | 5.7 | >50 |
| **118** | 5.29 | 3.96 | 4.48 | 5.44 | 3.07 | 6.26 | >20 |
| **119** | 5.54 | 4.28 | 2.86 | 5.65 | 2.44 | 5.22 | >20 |
| Etoposide | 0.30 | 1.06 | 0.76 | 1.53 | 0.63 | 1.05 | 11.73 |

[a]A549, lung cancer cells; HCT116, colon cancer cells; K562, leukemia cells; MDA-MB-231, breast cancer cells; SK-Hep-1, liver cancer cells; SNU638, stomach cancer cells; MRC5, lung normal epithelial cells.

Starting from Leu-AMS (**123**), Zhou et al.[135] reported the discovery of *N*-(4-sulfamoylphenyl)thioureas as a new class of *Trypanosoma brucei* LeuRS (*Tb*LeuRS) inhibitors (Fig. 22). Guided by molecular docking, simplified analogue **124** displayed good inhibitory activity against *Tb*LeuRS ($IC_{50}$ = 1.1 μmol/L), but its selectivity was poor (human cytoplasmic LeuRS $IC_{50}$ = 4.9 μmol/L). In 2018, Finn et al.[136] further simplified the scaffold (Fig. 22). Through analyzing the interaction between the inhibitors and the ATP binding site (Fig. 22B), benzenesulfonamide inhibitors were designed. The simplest analogue (**125**) was found to exhibit the best binding affinity against *E. coli* LeuRS with a $K_d$ value of 1.3 nmol/L. The antibacterial assay indicated that compound **125** showed moderate antibacterial activity against the *E. coli* ATCC 25922 strain (MIC = 8 μg/mL). Molecular docking simulation revealed that the amino and sulfamide groups of compound **125** formed three hydrogen bonds with residues Gln566, Met40 and Leu41 (Fig. 22C).

### 3.4. *Structural simplification by pharmacophore-based design*

#### 3.4.1. *Structural simplification of $SST_1$ receptor antagonists*

The somatostatin $SST_1$ receptors, members of the GPCR superfamily, act as inhibitory autoreceptors on somatostatin neurons in the hypothalamus, basal ganglia, retina and possibly hippocampus. $SST_1$ antagonists promote social interactions, reduce aggressive behavior and stimulate learning in rodents[138]. Through a systematic SAR study, obeline derivatives (**126**, Fig. 23) and ergoline (**127**, Fig. 23) were identified as highly potent and selective inhibitors of the $SST_1$ receptor ($K_d$ = 0.71 and 0.20 nmol/L, respectively). However, these compounds were difficult to synthesize and had poor pharmacokinetic properties. Through structural analysis, Troxler et al.[137] proposed that these ligands shared a common pharmacophore schematically represented by **128** (Fig. 23). Structural simplification was conducted based on this pharmacophore, and the chiral moiety was replaced with an achiral dibenzosuberane to afford analogue **129**, which retained the high $SST_1$ affinity ($K_d$ = 18.2 nmol/L) and selectivity over $SST_2$ (SI > 100) that was present in the parent compound. Further investigation was focused on the optimization of the tricyclic dibenzosuberane moiety, which led to the identification of novel, highly potent and selective $SST_1$ receptor antagonists[137]. Analogues **130** and **131** displayed the best $SST_1$ receptor antagonistic activities with $K_d$ values of 0.52 and 0.78 nmol/L, respectively. Moreover, these achiral analogues displayed favorable pharmacokinetic properties, namely, good oral absorption and metabolic stability, in rodents. In addition to good binding affinities, selectivities and PK profiles, these simplified analogues had better synthetic accessibility than the lead compounds and can be easily synthesized on a large scale.

#### 3.4.2. *Structural simplification of ATP synthase inhibitors*

Based on the binding mode of bedaquiline with ATP synthase (PDB code: 4V1F)[123], Saxena et al.[139] identified three important structural features in bedaquiline (Fig. 24), namely, the quinolone (**132**), tertiary amine (**133**) and hydroxyl fragments (**134**). Database searching and structure-based hit optimization led to compound **136** (Fig. 24), which displayed potent *in vitro* antituberculosis efficacy[139]. Moreover, it had good selectivity and favorable pharmacokinetic properties, such as quick absorption and distribution and slow elimination. Although compound **136** was not directly compared with bedaquiline, it has a relatively simpler structure and better synthetic accessibility and

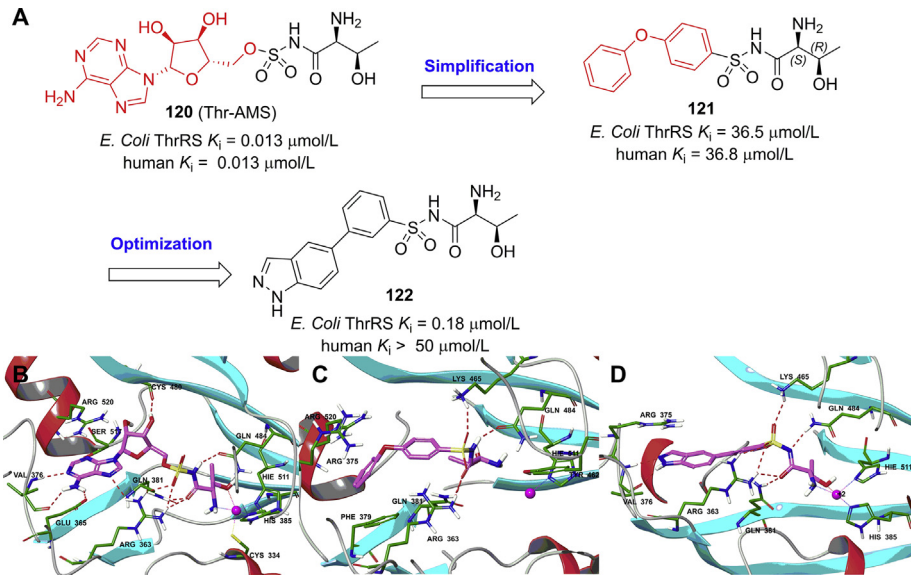


**Figure 21** Structural simplification of ThrRS inhibitors (A) and binding modes of **120** (B, PDB code: 1KOG), **121** (C) and **122** (D, PDB code: 4HWR) with *E. coli* ThrRS.

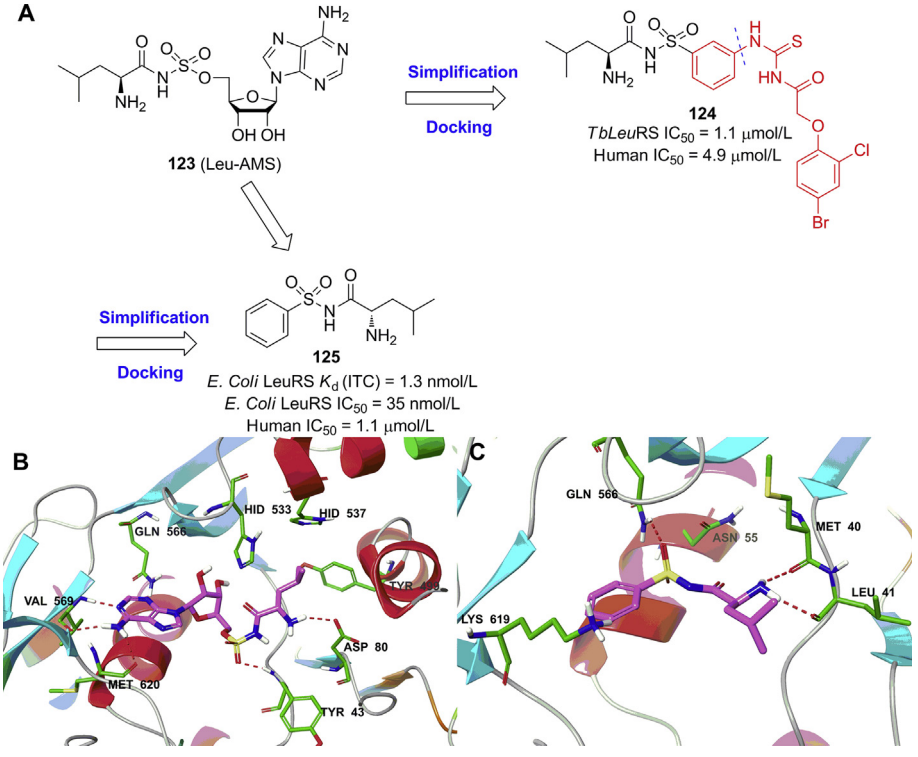


**Figure 22** Structural simplification of LeuRS inhibitors (A) and binding modes of **123** (B, PDB code: 5ONH), **125** (C) with *E. coli* LeuRS.

represents a promising preclinical candidate under further evaluations.

## 4. Conclusions and perspectives

Avoiding "molecular obesity" can improve the success rate of drug development. The design of "low-fat" drug-like molecules by structural simplification represents an effective strategy in lead optimization of both NPs and bioactive small molecules. Historically, structural simplification was initially applied in drug development to improve the synthetic accessibility and drug-likeness of complex NPs and successfully resulted in several marketed drugs. Recently, extremely complex NPs (*e.g.*, marine NPs) with highly potent biological activities have been identified, offering challenging targets for structural simplification. Thus, the development of efficient synthetic and

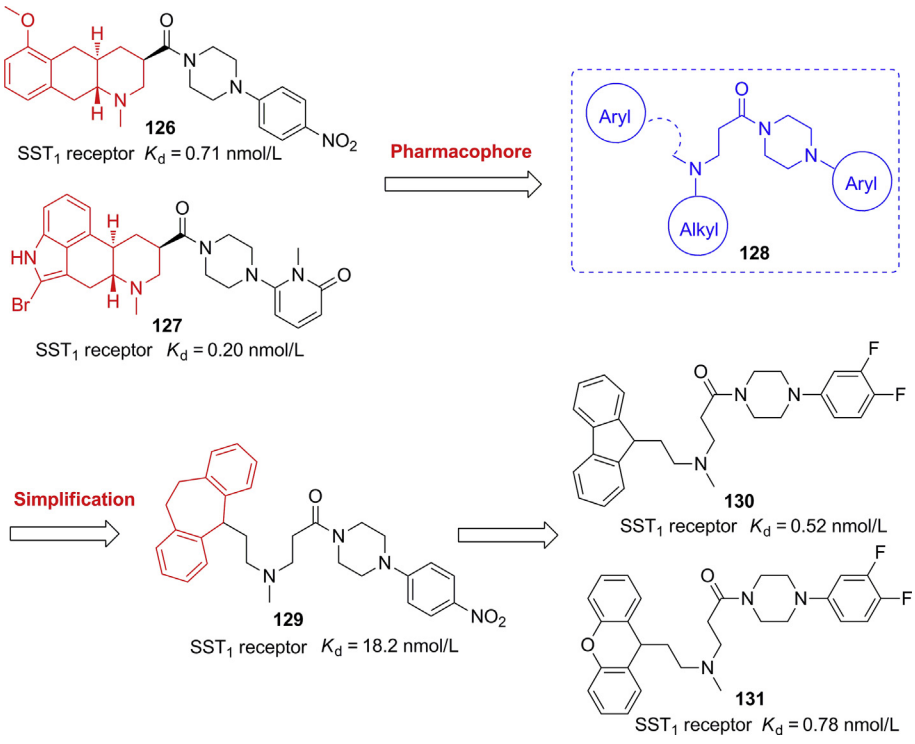


**Figure 23** Structural simplification of SST1 receptor antagonists.

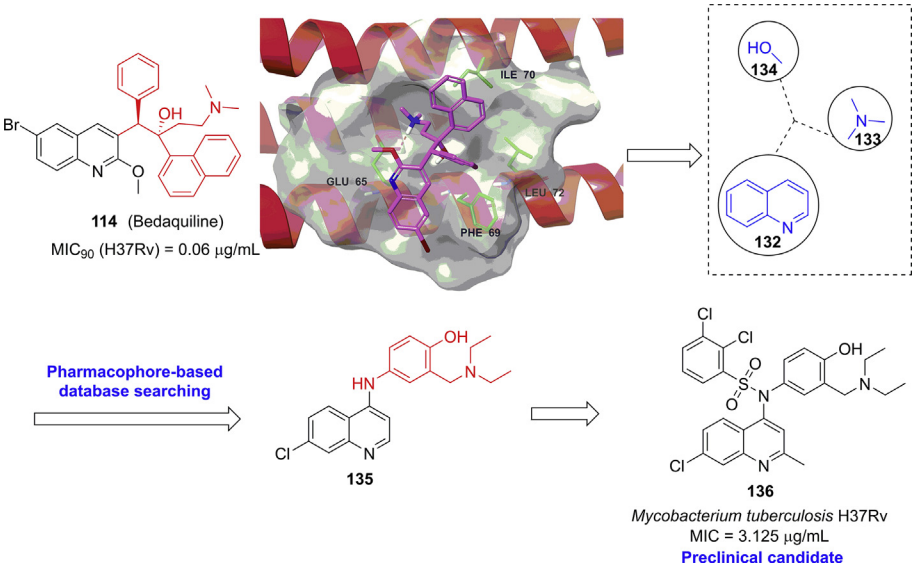


**Figure 24** Structural simplification of bedaquiline.

computational approaches for simplification design is highly desirable. For example, Scaffold Hunter[74] and BIOS provide efficient tools for the computational analysis of complex structures and bioactivity data and for identifying simplified scaffolds with the desired activity by rational fragmentation. Such new technologies will improve the efficiency of structural simplification.

Based on the numerous case studies described above, several guidelines can be summarized to guide future structural simplification studies. The first challenge is defining what constitutes a successful structural simplification study. Pharmacological activity is important but it is not the only criterion for evaluating the success of a simplified design. The identification of less complex molecules with comparable (or even with increased) biological activity is indeed the main goal for structural simplification. However, in some cases, the activity of the simplified compounds may be decreased, particularly at the molecular or cellular level. The value of simplification should be validated by more biological models, especially *in vivo* models, although most simplified analogues have not been fully assayed. Moreover, multiple rounds of

optimization are often required to improve the activity. Thus, the success of structural simplification should be defined based on whether the simplified compounds have addressed the drawbacks of the original lead compounds. The most important purpose of simplification is to improve the drug-likeness of lead compounds. Therefore, the balance among synthetic feasibility, *in vitro* and *in vivo* potency, physicochemical properties, and pharmacokinetic profiles should be considered. Moreover, structural simplification aims to design lead compounds or drug candidates with reduced synthetic difficulty, which will facilitate the development of synthetic process in the pharmaceutical industry. Second, during the simplification process, the biological activity and binding targets might change as the structure of the compound changes. Thus, moderate structural simplifications may be most appropriate. Finally, it is important to understand the scope of structural simplification, and not all bioactive compounds can be simplified. For some types of drug targets, the molecular complexity of the ligands is necessary to form unique and specific interactions, and the structural simplification of these molecules may be quite challenging. The construction of pharmacophore model is important to improve the efficiency of structural simplification design. Taken together, with the development of new design approaches and the increasing number of medicinal chemistry efforts devoted to this important area, structural simplification will play an important role in improving the efficiency and success rate of new drug development.

## Acknowledgments

This work was supported by the National Natural Science Foundation of China (Grant No. 81725020 to Chunquan Sheng and No. 21602252 to Shengzheng Wang), the Innovation Program of Shanghai Municipal Education Commission (Grant No. 2019-01-07-00-07-E00073 to Chunquan Sheng, China), and the Hong Kong Scholars Program (Grant No. XJ201713 to Shengzheng Wang, China).

## References

1. Mignani S, Huber S, Tomás H, Rodrigues J, Majoral JP. Compound high-quality criteria: a new vision to guide the development of drugs, current situation. *Drug Discov Today* 2016;**21**:573−84.
2. Polanski J, Bogocz J, Tkocz A. The analysis of the market success of FDA approvals by probing top 100 bestselling drugs. *J Comput Aided Mol Des* 2016;**30**:381−9.
3. Keserű GM, Makara GM. Hit discovery and hit-to-lead approaches. *Drug Discov Today* 2006;**11**:741−8.
4. Walters WP, Green J, Weiss JR, Murcko MA. What do medicinal chemists actually make? A 50-year retrospective. *J Med Chem* 2011;**54**:6405−16.
5. Oprea TI, Davis AM, Teague SJ, Leeson PD. Is there a difference between leads and drugs? A historical perspective. *J Chem Inf Comput Sci* 2001;**41**:1308−15.
6. Manly CJ, Chandrasekhar J, Ochterski JW, Hammer JD, Warfield BB. Strategies and tactics for optimizing the Hit-to-Lead process and beyond—a computational chemistry perspective. *Drug Discov Today* 2008;**13**:99−109.
7. Hann MM. Molecular obesity, potency and other addictions in drug discovery. *MedChemComm* 2011;**2**:349−55.
8. Hann MM, Keserü GM. Finding the sweet spot: the role of nature and nurture in medicinal chemistry. *Nat Rev Drug Discov* 2012;**11**:355−65.
9. Maynard AT, Roberts CD. Quantifying, visualizing, and monitoring lead optimization. *J Med Chem* 2016;**59**:4189−201.
10. Böttcher T. An additive definition of molecular complexity. *J Chem Inf Model* 2016;**56**:462−70.
11. Hann MM, Leach AR, Harper G. Molecular complexity and its impact on the probability of finding leads for drug discovery. *J Chem Inf Comput Sci* 2001;**41**:856−64.
12. Méndez-Lucio O, Medina-Franco JL. The many roles of molecular complexity in drug discovery. *Drug Discov Today* 2017;**22**:120−6.
13. Crane EA, Gademann K. Capturing biological activity in natural product fragments by chemical synthesis. *Angew Chem Int Ed Engl* 2016;**55**:3882−902.
14. Guo Z. The modification of natural products for medical use. *Acta Pharm Sin B* 2017;**7**:119−36.
15. Xiao Z, Morris-Natschke SL, Lee KH. Strategies for the optimization of natural leads to anticancer drugs or drug candidates. *Med Res Rev* 2016;**36**:32−91.
16. Rodrigues T, Reker D, Schneider P, Schneider G. Counting on natural products for drug design. *Nat Chem* 2016;**8**:531−41.
17. Blakemore PR, White JD. Morphine, the Proteus of organic molecules. *Chem Commun* 2002;**11**:1159−68.
18. Gudin J, Fudin J, Nalamachu S. Levorphanol use: past, present and future. *Postgrad Med* 2016;**128**:46−53.
19. Heel RC, Brogden RN, Speight TM, Avery GS. Butorphanol: a review of its pharmacological properties and therapeutic efficacy. *Drugs* 1978;**16**:473−505.
20. Commiskey S, Fan LW, Ho IK, Rockhold RW. Butorphanol: effects of a prototypical agonist-antagonist analgesic on $\kappa$-opioid receptors. *J Pharmacol Sci* 2005;**98**:109−16.
21. Aarnes TK, Muir III WW. Chapter 26—pain assessment and management. In: Peterson ME, Kutzler MA, editors. *Small animal pediatrics*. Saint Louis: W.B. Saunders; 2011. p. 220−32.
22. Prezzavento O, Arena E, Sánchez-Fernández C, Turnaturi R, Parenti C, Marrazzo A, et al. (+)- and (−)-Phenazocine enantiomers: evaluation of their dual opioid agonist/$\sigma_1$ antagonist properties and antinociceptive effects. *Eur J Med Chem* 2017;**125**:603−10.
23. Levine JD, Gordon NC. Synergism between the analgesic actions of morphine and pentazocine. *Pain* 1988;**33**:369−72.
24. Ziering A, Lee J. Piperidine derivatives. V. 1,3-Dialkyl-4-aryl-4-acyloxypiperidines. *J Org Chem* 1947;**12**:911−4.
25. Van Bever WF, Niemegeers CJ, Janssen PA. Synthetic analgesics. Synthesis and pharmacology of the diastereoisomers of *N*-[3-methyl-1-(2-phenylethyl)-4-piperidyl]-*N*-phenylpropanamide and *N*-[3-methyl-1-(1-methyl-2-phenylethyl)-4-piperidyl]-*N*-phenylpropanamide. *J Med Chem* 1974;**17**:1047−51.
26. Barnett CJ. Modification of methadone synthesis process step. US patent 4048211A. 1977 Sep 13.
27. King JA, Meltzer RI, Doczi J. The synthesis of some fluorene derivatives. *J Am Chem Soc* 1955;**77**:2217−23.
28. Corbett AD, Paterson SJ, Kosterlitz HW. Selectivity of ligands for opioid receptors. In: Herz A, Akil H, Simon EJ, editors. *Opioids*. Berlin, Heidelberg: Springer; 1993. p. 645−79.
29. Wang S, Dong G, Sheng C. Structural simplification of natural products. *Chem Rev* 2019;**119**:4180−220.
30. Uemura D, Takahashi K, Yamamoto T, Katayama C, Tanaka J, Okumura Y, et al. Norhalichondrin A: an antitumor polyether macrolide from a marine sponge. *J Am Chem Soc* 1985;**107**:4796−8.
31. Hirata Y, Uemura D. Halichondrins—antitumor polyether macrolides from a marine sponge. *Pure Appl Chem* 1986;**58**:701−10.
32. Bai RL, Paull KD, Herald CL, Malspeis L, Pettit GR, Hamel E. Halichondrin B and homohalichondrin B, marine natural products binding in the vinca domain of tubulin. Discovery of tubulin-based mechanism of action by analysis of differential cytotoxicity data. *J Biol Chem* 1991;**266**:15882−9.
33. Aicher TD, Buszek KR, Fang FG, Forsyth CJ, Jung SH, Kishi Y, et al. Total synthesis of halichondrin B and norhalichondrin B. *J Am Chem Soc* 1992;**114**:3162−4.
34. Jackson KL, Henderson JA, Phillips AJ. The halichondrins and E7389. *Chem Rev* 2009;**109**:3044−79.

35. Zheng W, Seletsky BM, Palme MH, Lydon PJ, Singer LA, Chase CE, et al. Macrocyclic ketone analogues of halichondrin B. *Bioorg Med Chem Lett* 2004;**14**:5551−4.
36. Towle MJ, Salvato KA, Budrow J, Wels BF, Kuznetsov G, Aalfs KK, et al. *In vitro* and *in vivo* anticancer activities of synthetic macrocyclic ketone analogues of halichondrin B. *Cancer Res* 2001;**61**:1013−21.
37. Donoghue M, Lemery SJ, Yuan W, He K, Sridhara R, Shord S, et al. Eribulin mesylate for the treatment of patients with refractory metastatic breast cancer: use of a "physician's choice" control arm in a randomized approval trial. *Clin Cancer Res* 2012;**18**:1496−505.
38. Fujita T, Hirose R, Hamamichi N, Kitao Y, Sasaki S, Yoneta M, et al. 2-Substituted 2-aminoethanol: minimum essential structure for immunosuppressive activity of ISP-I (myriocin). *Bioorg Med Chem Lett* 1995;**5**:1857−60.
39. Sasaki S, Hashimoto R, Kiuchi M, Inoue K, Ikumoto T, Hirose R, et al. Fungal metabolites. Part 14. Novel potent immunosuppressants, mycestericins, produced by *Mycelia sterilia*. *J Antibiot (Tokyo)* 1994;**47**:420−33.
40. Fujita T, Yoneta M, Hirose R, Sasaki S, Inoue K, Kiuchi M, et al. Simple compounds, 2-alkyl-2-amino-1,3-propanediols have potent immunosuppressive activity. *Bioorg Med Chem Lett* 1995;**5**:847−52.
41. Yoshida M, Horinouchi S, Beppu T. Trichostatin A and trapoxin: novel chemical probes for the role of histone acetylation in chromatin structure and function. *Bioessays* 1995;**17**:423−30.
42. Huang Y, Dong G, Li H, Liu N, Zhang W, Sheng C. Discovery of janus kinase 2 (JAK2) and histone deacetylase (HDAC) dual inhibitors as a novel strategy for the combinational treatment of leukemia and invasive fungal infections. *J Med Chem* 2018;**61**:6056−74.
43. Stowell JC, Huot RI, Van Voast L. The synthesis of *N*-hydroxy-*N*′-phenyloctanediamide and its inhibitory effect on proliferation of AXC rat prostate cancer cells. *J Med Chem* 1995;**38**:1411−3.
44. Mann BS, Johnson JR, Cohen MH, Justice R, Pazdur R. FDA approval summary: vorinostat for treatment of advanced primary cutaneous T-cell lymphoma. *Oncol* 2007;**12**:1247−52.
45. Liu GT. Bicyclol: a novel drug for treating chronic viral hepatitis B and C. *Med Chem* 2009;**5**:29−43.
46. Liu GT. Therapeutic effects of biphenyl dimethyl dicarboxylate (DDB) on chronic viral hepatitis B. *Proc Chin Acad Med Sci Peking Union Med Coll* 1987;**2**:228−33.
47. Liu GT. The anti-virus and hepatoprotective effect of bicyclol and its mechanism of action. *Chin J New Drugs* 2001;**10**:325−7.
48. Jirousek MR, Gillig JR, Gonzalez CM, Heath WF, McDonald III JH, Neel DA, et al. (*S*)-13-[(Dimethylamino)methyl]-10,11,14,15-tetrahydro-4,9:16,21-dimetheno-1*H*,13*H*-dibenzo[*e*,*k*]pyrrolo[3,4-*h*][1,4,13]oxadiazacyclohexadecene-1,3(2*H*)-dione (LY333531) and related analogues: isozyme selective inhibitors of protein kinase C$\beta$. *J Med Chem* 1996;**39**:2664−71.
49. Faul MM, Gillig JR, Jirousek MR, Ballas LM, Schotten T, Kahl A, et al. Acyclic *N*-(azacycloalkyl)bisindolylmaleimides: isozyme selective inhibitors of PKC$\beta$. *Bioorg Med Chem Lett* 2003;**13**:1857−9.
50. Chang RS, Lotti VJ, Monaghan RL, Birnbaum J, Stapley EO, Goetz MA, et al. A potent nonpeptide cholecystokinin antagonist selective for peripheral tissues isolated from *Aspergillus alliaceus*. *Science* 1985;**230**:177−9.
51. Zucker KA, Adrian TE, Zdon MJ, Ballantyne GH, Modlin IM. Asperlicin: a unique nonpeptide cholecystokinin antagonist. *Surgery* 1987;**102**:163−70.
52. Evans BE, Bock MG, Rittle KE, DiPardo RM, Whitter WL, Veber DF, et al. Design of potent, orally effective, nonpeptidal antagonists of the peptide hormone cholecystokinin. *Proc Natl Acad Sci U S A* 1986;**83**:4918−22.
53. Evans BE, Rittle KE, Bock MG, DiPardo RM, Freidinger RM, Whitter WL, et al. Design of nonpeptidal ligands for a peptide receptor: cholecystokinin antagonists. *J Med Chem* 1987;**30**:1229−39.
54. Evans BE, Rittle KE, Bock MG, DiPardo RM, Freidinger RM, Whitter WL, et al. Methods for drug discovery: development of potent, selective, orally effective cholecystokinin antagonists. *J Med Chem* 1988;**31**:2235−46.
55. Weber L. The application of multi-component reactions in drug discovery. *Curr Med Chem* 2002;**9**:2085−93.
56. Magedov IV, Frolova L, Manpadi M, Bhoga UD, Tang H, Evdokimov NM, et al. Anticancer properties of an important drug lead podophyllotoxin can be efficiently mimicked by diverse heterocyclic scaffolds accessible *via* one-step synthesis. *J Med Chem* 2011;**54**:4234−46.
57. Evdokimov NM, Van Slambrouck S, Heffeter P, Tu L, Le Calvé B, Lamoral-Theys D, et al. Structural simplification of bioactive natural products with multicomponent synthesis. 3. Fused uracil-containing heterocycles as novel topoisomerase-targeting agents. *J Med Chem* 2011;**54**:2012−21.
58. Magedov IV, Manpadi M, Ogasawara MA, Dhawan AS, Rogelj S, Van Slambrouck S, et al. Structural simplification of bioactive natural products with multicomponent synthesis. 2. Antiproliferative and antitubulin activities of pyrano[3,2-*c*]pyridones and pyrano[3,2-*c*]quinolones. *J Med Chem* 2008;**51**:2561−70.
59. Soria-Mercado IE, Prieto-Davo A, Jensen PR, Fenical W. Antibiotic terpenoid chloro-dihydroquinones from a new marine actinomycete. *J Nat Prod* 2005;**68**:904−10.
60. Hussain H, Krohn K, Ahmad VU, Miana GA. Green IR. Lapachol: an overview. *Arkivoc* 2007;**2**:145−71.
61. Siripong P, Kanokmedakul K, Piyaviriyagul S, Yahuafai J, Chanpai R, Ruchirawat S, et al. Antiproliferative naphthoquinone esters from *Rhinacanthus nasutus* Kurz. roots on various cancer cells. *J Tradit Med* 2006;**23**:166−72.
62. Magedov IV, Kireev AS, Jenkins AR, Evdokimov NM, Lima DT, Tongwa P, et al. Structural simplification of bioactive natural products with multicomponent synthesis. 4. 4*H*-pyrano-[2,3-*b*]naphthoquinones with anticancer activity. *Bioorg Med Chem Lett* 2012;**22**:5195−8.
63. Over B, Wetzel S, Grütter C, Nakai Y, Renner S, Rauh D, et al. Natural-product-derived fragments for fragment-based ligand discovery. *Nat Chem* 2013;**5**:21−8.
64. Grabowski K, Baringhaus KH, Schneider G. Scaffold diversity of natural products: inspiration for combinatorial library design. *Nat Prod Rep* 2008;**25**:892−904.
65. Bon RS, Waldmann H. Bioactivity-guided navigation of chemical space. *Acc Chem Res* 2010;**43**:1103−14.
66. Lachance H, Wetzel S, Kumar K, Waldmann H. Charting, navigating, and populating natural product chemical space for drug discovery. *J Med Chem* 2012;**55**:5989−6001.
67. Barelier S, Eidam O, Fish I, Hollander J, Figaroa F, Nachane R, et al. Increasing chemical space coverage by combining empirical and computational fragment screens. *ACS Chem Biol* 2014;**9**:1528−35.
68. Reutlinger M, Rodrigues T, Schneider P, Schneider G. Multi-objective molecular *de novo* design by adaptive fragment prioritization. *Angew Chem Int Ed Engl* 2014;**53**:4244−8.
69. Jin X, Lee K, Kim NH, Kim HS, Yook JI, Choi J, et al. Natural products used as a chemical library for protein–protein interaction targeted drug discovery. *J Mol Graph Model* 2018;**79**:46−58.
70. Koch MA, Schuffenhauer A, Scheck M, Wetzel S, Casaulta M, Odermatt A, et al. Charting biologically relevant chemical space: a structural classification of natural products (SCONP). *Proc Natl Acad Sci U S A* 2005;**102**:17272−7.
71. Schuffenhauer A, Ertl P, Roggo S, Wetzel S, Koch MA, Waldmann H. The scaffold tree—visualization of the scaffold universe by hierarchical scaffold classification. *J Chem Inf Model* 2007;**47**:47−58.
72. Balamurugan R, Dekker FJ, Waldmann H. Design of compound libraries based on natural product scaffolds and protein structure similarity clustering (PSSC). *Mol Biosyst* 2005;**1**:36−45.
73. Renner S, van Otterlo WA, Dominguez Seoane MD, Möcklinghoff S, Hofmann B, Wetzel S, et al. Bioactivity-guided mapping and navigation of chemical space. *Nat Chem Biol* 2009;**5**:585−92.

74. Wetzel S, Klein K, Renner S, Rauh D, Oprea TI, Mutzel P, et al. Interactive exploration of chemical space with Scaffold Hunter. *Nat Chem Biol* 2009;**5**:581−3.
75. Prescher H, Koch G, Schuhmann T, Ertl P, Bussenault A, Glick M, et al. Construction of a 3D-shaped, natural product like fragment library by fragmentation and diversification of natural products. *Bioorg Med Chem* 2017;**25**:921−5.
76. Wetzel S, Bon RS, Kumar K, Waldmann H. Biology-oriented synthesis. *Angew Chem Int Ed Engl* 2011;**50**:10800−26.
77. van Hattum H, Waldmann H. Biology-oriented synthesis: harnessing the power of evolution. *J Am Chem Soc* 2014;**136**:11853−9.
78. Laraia L, Waldmann H. Natural product inspired compound collections: evolutionary principle, chemical synthesis, phenotypic screening, and target identification. *Drug Discov Today Technol* 2017;**23**:75−82.
79. Galliford CV, Scheidt KA. Pyrrolidinyl-spirooxindole natural products as inspirations for the development of potential therapeutic agents. *Angew Chem Int Ed Engl* 2007;**46**:8748−58.
80. Antonchick AP, Gerding-Reimers C, Catarinella M, Schürmann M, Preut H, Ziegler S, et al. Highly enantioselective synthesis and cellular evaluation of spirooxindoles inspired by natural products. *Nat Chem* 2010;**2**:735−40.
81. Funel-Le Bon C, Berrué F, Thomas OP, Reyes F, Amade P, Sodwanone S. A triterpene from the marine sponge *Axinella weltneri*. *J Nat Prod* 2005;**68**:1284−7.
82. Basu S, Ellinger B, Rizzo S, Deraeve C, Schürmann M, Preut H, et al. Biology-oriented synthesis of a natural-product inspired oxepane collection yields a small-molecule activator of the Wnt-pathway. *Proc Natl Acad Sci U S A* 2011;**108**:6805−10.
83. Orosz F, Horvath I, Ovadi J. New anti-mitotic drugs with distinct anti-calmodulin activity. *Mini Rev Med Chem* 2006;**6**:1145−57.
84. Dückert H, Pries V, Khedkar V, Menninger S, Bruss H, Bird AW, et al. Natural product-inspired cascade synthesis yields modulators of centrosome integrity. *Nat Chem Biol* 2011;**8**:179−84.
85. Peyssonnaux C, Eychène A. The Raf/MEK/ERK pathway: new concepts of activation. *Biol Cell* 2001;**93**:53−62.
86. Davies H, Bignell GR, Cox C, Stephens P, Edkins S, Clegg S, et al. Mutations of the BRAF gene in human cancer. *Nature* 2002;**417**:949−54.
87. Singer G, Oldt III R, Cohen Y, Wang BG, Sidransky D, Kurman RJ, et al. Mutations in BRAF and KRAS characterize the development of low-grade ovarian serous carcinoma. *J Natl Cancer Inst* 2003;**95**:484−6.
88. Tsai J, Lee JT, Wang W, Zhang J, Cho H, Mamo S, et al. Discovery of a selective inhibitor of oncogenic B-Raf kinase with potent antimelanoma activity. *Proc Natl Acad Sci U S A* 2008;**105**:3041−6.
89. Stellwagen JC, Adjabeng GM, Arnone MR, Dickerson SH, Han C, Hornberger KR, et al. Development of potent B-Raf$^{V600E}$ inhibitors containing an arylsulfonamide headgroup. *Bioorg Med Chem Lett* 2011;**21**:4436−40.
90. Rheault TR, Stellwagen JC, Adjabeng GM, Hornberger KR, Petrov KG, Waterson AG, et al. Discovery of dabrafenib: a selective inhibitor of Raf kinases with antitumor activity against B-Raf-driven Tumors. *ACS Med Chem Lett* 2013;**4**:358−62.
91. Zhang C, Spevak W, Zhang Y, Burton EA, Ma Y, Habets G, et al. RAF inhibitors that evade paradoxical MAPK pathway activation. *Nature* 2015;**526**:583−6.
92. Wright CJ, McCormack PL. Trametinib: first global approval. *Drugs* 2013;**73**:1245−54.
93. Johnston JA, Bacon CM, Riedy MC, O'Shea JJ. Signaling by IL-2 and related cytokines: JAKs, STATs, and relationship to immunodeficiency. *J Leukoc Biol* 1996;**60**:441−52.
94. Flanagan ME, Blumenkopf TA, Brissette WH, Brown MF, Casavant JM, Shang-Poa C, et al. Discovery of CP-690,550: a potent and selective Janus kinase (JAK) inhibitor for the treatment of autoimmune diseases and organ transplant rejection. *J Med Chem* 2010;**53**:8468−84.
95. Russell SM, Tayebi N, Nakajima H, Riedy MC, Roberts JL, Aman MJ, et al. Mutation of Jak3 in a patient with SCID: essential role of Jak3 in lymphoid development. *Science* 1995;**270**:797−800.
96. Changelian PS, Flanagan ME, Ball DJ, Kent CR, Magnuson KS, Martin WH, et al. Prevention of organ allograft rejection by a specific Janus kinase 3 inhibitor. *Science* 2003;**302**:875−8.
97. Millan MJ. *N*-Methyl-D-aspartate receptors as a target for improved antipsychotic agents: novel insights and clinical perspectives. *Psychopharmacology* 2005;**179**:30−53.
98. Bergeron R, Meyer TM, Coyle JT, Greene RW. Modulation of *N*-methyl-D-aspartate receptor function by glycine transport. *Proc Natl Acad Sci U S A* 1998;**95**:15730−4.
99. Jolidon S, Alberati D, Dowle A, Fischer H, Hainzl D, Narquizian R, et al. Design, synthesis and structure–activity relationship of simple bis-amides as potent inhibitors of GlyT1. *Bioorg Med Chem Lett* 2008;**18**:5533−6.
100. Tepper SJ, Stillman MJ. Clinical and preclinical rationale for CGRP-receptor antagonists in the treatment of migraine. *Headache* 2008;**48**:1259−68.
101. Ho TW, Ferrari MD, Dodick DW, Galet V, Kost J, Fan X, et al. Efficacy and tolerability of MK-0974 (telcagepant), a new oral antagonist of calcitonin gene-related peptide receptor, compared with zolmitriptan for acute migraine: a randomised, placebo-controlled, parallel-treatment trial. *Lancet* 2008;**372**:2115−23.
102. Wood MR, Schirripa KM, Kim JJ, Quigley AG, Stump CA, Bell IM, et al. Novel CGRP receptor antagonists through a design strategy of target simplification with addition of molecular flexibility. *Bioorg Med Chem Lett* 2009;**19**:5787−90.
103. Paone DV, Shaw AW, Nguyen DN, Burgey CS, Deng JZ, Kane SA, et al. Potent, orally bioavailable calcitonin gene-related peptide receptor antagonists for the treatment of migraine: discovery of *N*-[(3*R*,6*S*)-6-(2,3-difluorophenyl)-2-oxo-1-(2,2,2-trifluoroethyl)azepan-3-yl]-4-(2-oxo-2,3-dihydro-1*H*-imidazo[4,5-*b*]pyridin-1-yl) piperidine-1-carboxamide (MK-0974). *J Med Chem* 2007;**50**:5564−7.
104. Manetti D, Ghelardini C, Bartolini A, Bellucci C, Dei S, Galeotti N, et al. Design, synthesis, and preliminary pharmacological evaluation of 1,4-diazabicyclo[4.3.0]nonan-9-ones as a new class of highly potent nootropic agents. *J Med Chem* 2000;**43**:1969−74.
105. Manetti D, Ghelardini C, Bartolini A, Dei S, Galeotti N, Gualtieri F, et al. Molecular simplification of 1,4-diazabicyclo[4.3.0]nonan-9-ones gives piperazine derivatives that maintain high nootropic activity. *J Med Chem* 2000;**43**:4499−507.
106. Lenzi O, Colotta V, Catarzi D, Varano F, Filacchioni G, Martini C, et al. 4-Amido-2-aryl-1,2,4-triazolo[4,3-*a*]quinoxalin-1-ones as new potent and selective human $A_3$ adenosine receptor antagonists. Synthesis, pharmacological evaluation, and ligand-receptor modeling studies. *J Med Chem* 2006;**49**:3916−25.
107. Morizzo E, Capelli F, Lenzi O, Catarzi D, Varano F, Filacchioni G, et al. Scouting human $A_3$ adenosine receptor antagonist binding mode using a molecular simplification approach: from triazoloquinoxaline to a pyrimidine skeleton as a key study. *J Med Chem* 2007;**50**:6596−606.
108. Poli D, Catarzi D, Colotta V, Varano F, Filacchioni G, Daniele S, et al. The identification of the 2-phenylphthalazin-1(2*H*)-one scaffold as a new decorable core skeleton for the design of potent and selective human $A_3$ adenosine receptor antagonists. *J Med Chem* 2011;**54**:2102−13.
109. Colotta V, Catarzi D, Varano F, Capelli F, Lenzi O, Filacchioni G, et al. New 2-arylpyrazolo[3,4-*c*]quinoline derivatives as potent and selective human $A_3$ adenosine receptor antagonists. Synthesis, pharmacological evaluation, and ligand–receptor modeling studies. *J Med Chem* 2007;**50**:4061−74.

110. Lenzi O, Colotta V, Catarzi D, Varano F, Poli D, Filacchioni G, et al. 2-Phenylpyrazolo[4,3-*d*]pyrimidin-7-one as a new scaffold to obtain potent and selective human $A_3$ adenosine receptor antagonists: new insights into the receptor-antagonist recognition. *J Med Chem* 2009; **52**:7640−52.
111. Cheong SL, Dolzhenko A, Kachler S, Paoletta S, Federico S, Cacciari B, et al. The significance of 2-furyl ring substitution with a 2-(*para*-substituted) aryl group in a new series of pyrazolo-triazolo-pyrimidines as potent and highly selective $hA_3$ adenosine receptors antagonists: new insights into structure–affinity relationship and receptor-antagonist recognition. *J Med Chem* 2010;**53**:3361−75.
112. Venkatesan G, Paira P, Cheong SL, Vamsikrishna K, Federico S, Klotz KN, et al. Discovery of simplified $N^2$-substituted pyrazolo[3,4-*d*]pyrimidine derivatives as novel adenosine receptor antagonists: efficient synthetic approaches, biological evaluations and molecular docking studies. *Bioorg Med Chem* 2014;**22**:1751−65.
113. Barr SC, Warner KL, Kornreic BG, Piscitelli J, Wolfe A, Benet L, et al. A cysteine protease inhibitor protects dogs from cardiac damage during infection by *Trypanosoma cruzi*. *Antimicrob Agents Chemother* 2005;**49**:5160−1.
114. Ferreira RS, Simeonov A, Jadhav A, Eidam O, Mott BT, Keiser MJ, et al. Complementarity between a docking and a high-throughput screen in discovering new cruzain inhibitors. *J Med Chem* 2010;**53**:4891−905.
115. Braga SF, Martins LC, da Silva EB, Sales Junior PA, Murta SM, Romanha AJ, et al. Synthesis and biological evaluation of potential inhibitors of the cysteine proteases cruzain and rhodesain designed by molecular simplification. *Bioorg Med Chem* 2017;**25**:1889−900.
116. Montagnoli A, Tenca P, Sola F, Carpani D, Brotherton D, Albanese C, et al. Cdc7 inhibition reveals a p53-dependent replication checkpoint that is defective in cancer cells. *Cancer Res* 2004;**64**: 7110−6.
117. Swords R, Mahalingam D, O'Dwyer M, Santocanale C, Kelly K, Carew J, et al. Cdc7 kinase—a new target for drug development. *Eur J Cancer* 2010;**46**:33−40.
118. Vanotti E, Amici R, Bargiotti A, Berthelsen J, Bosotti R, Ciavolella A, et al. Cdc7 kinase inhibitors: pyrrolopyridinones as potential antitumor agents. 1. Synthesis and structure–activity relationships. *J Med Chem* 2008;**51**:487−501.
119. Hughes S, Elustondo F, Di Fonzo A, Leroux FG, Wong AC, Snijders AP, et al. Crystal structure of human CDC7 kinase in complex with its activator DBF4. *Nat Struct Mol Biol* 2012;**19**:1101−7.
120. Menichincheri M, Bargiotti A, Berthelsen J, Bertrand JA, Bossi R, Ciavolella A, et al. First Cdc7 kinase inhibitors: pyrrolopyridinones as potent and orally active antitumor agents. 2. Lead discovery. *J Med Chem* 2009;**52**:293−307.
121. Menichincheri M, Albanese C, Alli C, Ballinari D, Bargiotti A, Caldarelli M, et al. Cdc7 kinase inhibitors: 5-heteroaryl-3-carboxamido-2-aryl pyrroles as potential antitumor agents. 1. Lead finding. *J Med Chem* 2010;**53**:7296−315.
122. Mahajan R. Bedaquiline: first FDA-approved tuberculosis drug in 40 years. *Int J Appl Basic Med Res* 2013;**3**:1−2.
123. Preiss L, Langer JD, Yildiz Ö, Eckhardt-Strelau L, Guillemont JE, Koul A, et al. Structure of the mycobacterial ATP synthase $F_o$ rotor ring in complex with the anti-TB drug bedaquiline. *Sci Adv* 2015;**1**: e1500106.
124. He C, Preiss L, Wang B, Fu L, Wen H, Zhang X, et al. Structural simplification of bedaquiline: the discovery of 3-(4-(*N,N*-dimethylaminomethyl)phenyl)quinoline-derived antitubercular lead compounds. *ChemMedChem* 2017;**12**:106−19.
125. Bonfils G, Jaquenoud M, Bontron S, Ostrowicz C, Ungermann C, De Virgilio C. Leucyl-tRNA synthetase controls TORC1 *via* the EGO complex. *Mol Cell* 2012;**46**:105−10.
126. Han JM, Jeong SJ, Park MC, Kim G, Kwon NH, Kim HK, et al. Leucyl-tRNA synthetase is an intracellular leucine sensor for the mTORC1-signaling pathway. *Cell* 2012;**149**:410−24.
127. Yoon S, Kim JH, Kim SE, Kim C, Tran PT, Ann J, et al. Discovery of leucyladenylate sulfamates as novel leucyl-tRNA synthetase (LRS)-targeted mammalian target of rapamycin complex 1 (mTORC1) inhibitors. *J Med Chem* 2016;**59**:10322−8.
128. Yoon S, Kim JH, Koh Y, Tran PT, Ann J, Yoon I, et al. Discovery of simplified leucyladenylate sulfamates as novel leucyl-tRNA synthetase (LRS)-targeted mammalian target of rapamycin complex 1 (mTORC1) inhibitors. *Bioorg Med Chem* 2017;**25**:4145−52.
129. Hurdle JG, O'Neill AJ, Chopra I. Prospects for aminoacyl-tRNA synthetase inhibitors as new antimicrobial agents. *Antimicrob Agents Chemother* 2005;**49**:4821−33.
130. Cochrane RV, Norquay AK, Vederas JC. Natural products and their derivatives as tRNA synthetase inhibitors and antimicrobial agents. *MedChemComm* 2016;**7**:1535−45.
131. Vondenhoff GH, Van Aerschot A. Aminoacyl-tRNA synthetase inhibitors as potential antibiotics. *Eur J Med Chem* 2011;**46**: 5227−36.
132. Silvian LF, Wang J, Steitz TA. Insights into editing from an ile-tRNA synthetase structure with $tRNA^{ile}$ and mupirocin. *Science* 1999;**285**: 1074−7.
133. Teng M, Hilgers MT, Cunningham ML, Borchardt A, Locke JB, Abraham S, et al. Identification of bacteria-selective threonyl-tRNA synthetase substrate inhibitors by structure-based design. *J Med Chem* 2013;**56**:1748−60.
134. Torres-Larios A, Dock-Bregeon AC, Romby P, Rees B, Sankaranarayanan R, Caillet J, et al. Structural basis of translational control by *Escherichia coli* threonyl tRNA synthetase. *Nat Struct Biol* 2002;**9**:343−7.
135. Zhang F, Du J, Wang Q, Hu Q, Zhang J, Ding D, et al. Discovery of *N*-(4-sulfamoylphenyl)thioureas as *Trypanosoma brucei* leucyl-tRNA synthetase inhibitors. *Org Biomol Chem* 2013;**11**:5310−24.
136. Charlton MH, Aleksis R, Saint-Leger A, Gupta A, Loza E, Ribas de Pouplana L, et al. *N*-Leucinyl benzenesulfonamides as structurally simplified leucyl-tRNA synthetase inhibitors. *ACS Med Chem Lett* 2018;**9**:84−8.
137. Troxler T, Hurth K, Mattes H, Prashad M, Schoeffter P, Langenegger D, et al. Discovery of novel non-peptidic $\beta$-alanine piperazine amide derivatives and their optimization to achiral, easily accessible, potent and selective somatostatin $sst_1$ receptor antagonists. *Bioorg Med Chem Lett* 2009;**19**:1305−9.
138. Hoyer D, Nunn C, Hannon J, Schoeffter P, Feuerbach D, Schuepbach E, et al. SRA880, *in vitro* characterization of the first non-peptide somatostatin $sst_1$ receptor antagonist. *Neurosci Lett* 2004;**361**:132−5.
139. Singh S, Roy KK, Khan SR, Kashyap VK, Sharma A, Jaiswal S, et al. Novel, potent, orally bioavailable and selective mycobacterial ATP synthase inhibitors that demonstrated activity against both replicating and non-replicating. *M. tuberculosis*. *Bioorg Med Chem* 2015;**23**:742−52.